Graduate School of Frontier Sciences, The University of Tokyo

Department of Socio-cultural Environmental Studies

2008-2009

Master's Thesis

Influence of Rainfall and Combined Sewerage Overflow on Odaiba Area in Tokyo Bay

Submitted: July, 2009

Advisor
Asst. Prof. Yukio Koibuchi

076957 M. M. Majedul Islam

2008-2009 Master's Thesis

Influence of Rainfall and Combined Sewerage Overflow on Odaiba Area in Tokyo Bay

M. M. Majedul Islam

A THESIS SUBMITTED IN PARTIAL FULFILLMENT OF THE REQUIREMENTS FOR THE DEGREE OF MASTER'S OF SCIENCE IN ENVIRONMENTAL STUDIES

Department of Socio-cultural Environmental Studies,
Graduate School of Frontier Sciences
The University of Tokyo

31 July, 2009

ABSTRACT

The primary objective of this study was to identify the influence of rainfall induced overflowed sewer on Tokyo Bay water quality. To attain the objective emphasis was given to numerical simulation using mainly *E. coli* and Adenovirus as an indicator. Due to difficulties in intensive monitoring, field study was done just 5 days in November 2007 after an antecedent rainfall. But that data was not sufficient to validate the numerical model. So to validate the model a secondary observation data of 2004 was used. The observation result during the present field study in 2007 was used only to understand the general trend and as a supportive data to discuss the research outcomes.

From the observed data it was found that water quality parameters, water nutrients and pathogen level in the water column were highly affected after rainfall. After a storm effect the pathogen level in water column increased significantly and in most cases it surpluses the environmental quality standard for coastal water. Observed data after a rain event show a significant relative increase in the pathogen contamination in the Bay water, near to the mouth of Sumida River and adjacent area of STPs. The higher plume remains two to five days after the beginning of the runoff. There are many factors that play a role in the pathogen contamination at the mouth of the river. These include, but are not limited to, rainfall intensity, river flow, tidal level and wind direction and speed.

Frequent sampling and intensive monitoring is required to characterize the dynamics and distribution of contaminants adequately. But that is virtually very difficult and nearly impossible. To avoid this, a three dimensional hydrodynamic, water quality model coupled with a pathogen model was used. The simulations were done with two nested domains. The first domain covers the whole bay (grid size was 2km) and the second domains for only Odaiba area using a higher resolution (grid size 100m) with 10 sigma layers. The model was calibrated and validated using observed secondary data. The model performs well in predicting pathogen plumes resulting from the stormwater discharges to the shore area of Odaiba. Field observations for Fecal Coliforms in storm water outfall plumes indicate that the model predicted pathogen concentrations are reasonable. The upper limits predicted by the model and those measured in the field are in good agreement. The model results show the typical two to three-day wet weather effect of stormwater discharges where as observed data shows that the effects remain longer in surface water.

Storm induced discharge from river and pumping stations and influence of tide and current was identified as the dominant factor. The distributions and dynamics of pathogen were found very complex. Modeling result shows that high pathogen levels are not necessarily tied with amount of rainfall. Even in small precipitations, pathogen concentration can increase significantly. These kinds of results would be impossible to understand only from observation. The model successfully captured complex distributions of pathogen and helped our understanding of pathogens contaminations.

This study demonstrated the utility of hydrodynamic and water quality modeling for predicting spatial and temporal patterns of pathogen in the coastal water. The factors affecting pathogen concentration will vary from system to system, but this study demonstrated that pathogen distribution and patterns can be explained using present modeling technology. This technology can be considered as a potential alternative to monitoring, in managing coastal water.

As, big storm event is not so frequent and loadings from bigger storms usually represent only a small fraction of the total annual CSO, relatively smaller size of low cost storage reservoir can be effective to address most of the CSO problem caused by small and frequent storm events. For big storm case, swimming should be avoided until at least 3 days following a big storm.

ACKNOWLEDGEMENTS

First of all, all my appreciation and indebtedness go for the creator of the universe, the omnipotent, omniscient, omnipresent Allah for overcoming all the difficulties that I faced during this study and for being able to complete this thesis.

I am delighted to express my deepest sense of gratitude, sincerest indebtedness and profound respect to my supervisor Dr. Yukio Koibuchi, Assistant Professor, Department of Socio-cultural Environmental Studies, Graduate School of Frontier Science, The University of Tokyo. He guided me scholastically during my research period and provided suggestions and criticism to execute this thesis successfully. I am grateful to him for sharing his profound knowledge, experience and vision in the field of coastal engineering during our discussions.

Special thanks are extended to Professor Masahiko Isobe, and Associate Professor Dr. Huang Guangwei, Department of Socio-cultural Environmental Studies, Graduate School of Frontier Science, The University of Tokyo for their continuous guidance and instructions during this study and also for their comments and suggestions during lab-seminars.

I express my gratitude to, Dr. H. Satoh, Associate Professor, and Dr. S. Tsuji, Professor, Graduate School of Frontier Science, The University of Tokyo for their comments and suggestions as my co-supervisor.

I sincerely acknowledge the contributions of Professor Furumai and fellows of his Lab for providing me with various observation data and suggestions.

My sincere thanks to Mr. Keiichi Onozawa, former student for helping me with numerical modeling and providing observation data.

I would like to thank all of my lab mates who helped me during field observation and laboratory analysis. I appreciate Mr. Ariyo Kanno, Doctor student, for his help regarding the numerical work.

Special thanks to Mr. Munetoshi Kondoh, former master's student, who was assigned as my tutor, for his continuous supports that he provided me after my arrival in Japan. He also assisted me with nutrient Auto Analyzer and many research related and nonrelated stuffs. I am ever grateful to him for his assistances.

My hearty thanks go to all of my contemporary lab mates and former students specially Mrs. Merry Kimura, Dr. Kazumi Terada, Mr. Mutahara Mr. Oshiro, Mr. Satoh, Mr. Shinohara, Mr. Kakiuchi and Mrs. Miura.

I again acknowledge my lab-mates Mrs. Merry Kimura and Mr. Munetoshi Kondoh for their helps related to language matters in my research and oral communications with others. I sincerely thank the Japanese Language Teachers and Foreign Student Officers.

I acknowledge my parents whose prayer and advice are always with me in this tough course of life. I also would like to convey special thanks to all my teachers, friends and well wishers for their kind co-operation, encouragement and inspiration to complete this thesis.

I would like to express my sincere gratitude to the University of Tokyo and Asian Development Bank-Japan for providing such a great opportunity to pursue me the MS Degree.

At last, I would like to admit that whatever the success of this study is due for Almighty Allah, my supervisor and teachers and whatever the errors and faults are all mines.

Thank you! July 31, 2009

TABLE of CONTENTS

LIST OF TABLES

LIST OF FIGURES

Continued……

Continued……

LIST OF ABBREVIATIONS

Abbreviation	Elaboration
DO	Dissolved Oxygen
^{0}C	Degree Celsius
NTU	Nephelometric Turbidity Units
SS	Suspended Solids
TOC	Total Organic Curbon
pH	− log10 [H+] (Potential of Hydrogen)
CSO	Combined Sewerage Overflow
FIB	Fecal Indicator Bacteria
E. coli	*Escherichia Coli*
AdV	Adenovirus
STP	Sewage Treatment Plant
WRC	Water Reclamation Centre
RWI	Recreational Water Illness
US EPA	United States Environmental Protection Agency
TN	Total Nitrogen
TP	Total Phosphorus
TMG	Tokyo Metropolitan Government
NPS	Non Point Source
CFU	Colony Forming Unit
ECOMSED	Estuarine, Coastal and Ocean Modeling System with Sediments

CHAPTER 1: INTRODUCTION

1.1 General

Coastal zones contain rich resources to produce goods and services and are home to most commercial and industrial activities. Many big cities of the world are located near coastal zones which is a dynamic area of natural change and of increasing human use. It is estimated that nearly two-thirds of the world's population lives within 100 miles of an ocean, inland sea or major freshwater lake and three-quarters of the world population expected to reside in the coastal zone by 2025 (Gommes, *et. al*., 1998). Human activities impose an enormous amount of pressures on coastal zones.

Tokyo Bay is a semi-enclosed coastal sea, surrounded by one of the world's most urbanized areas (the Tokyo Metropolitan area) with a population of approximately 26 million. Annually, approximately 2 km^3 of sewage effluents drain into the inner part of the bay directly or via rivers (Managaki *et. al*., 2006). Thus, Tokyo Bay receives enormous pollutant load via both sewers and rivers and is considered the most polluted bay of Japan. Effluents released into the bay water pose a risk of pathogen contamination and human disease. This risk is increased for Tokyo Bay as it receives Combined Sewer Overflows (CSO's) during storms.

Tokyo's Bureau of Sewerage employs a combined system in which both storm water and sanitary waters are flows through the same pipelines. During storms, enormous amounts of raw sewage have been overflowing directly into Tokyo Bay without being treated at the Sewage Treatment Plants (STPs). Because the transient but vast amounts of waste water during storms exceeds the capacity of sewerage system.

1.2 What is a Combined Sewer Overflow?

A CSO is a discharge from a combined sewer system directly into a waterway. A combined sewer system is designed to collect a mixture of rainfall runoff, domestic and industrial wastewater in the same pipe for conveyance to a wastewater treatment plant (MWRDGC, 2006).

A CSO may occur during heavy rainfalls when the inflow of combined wastewater exceeds the capacity of the combined sewer system and the wastewater treatment plant. Figure 1.1 shows the combined and separated type of sewer system.

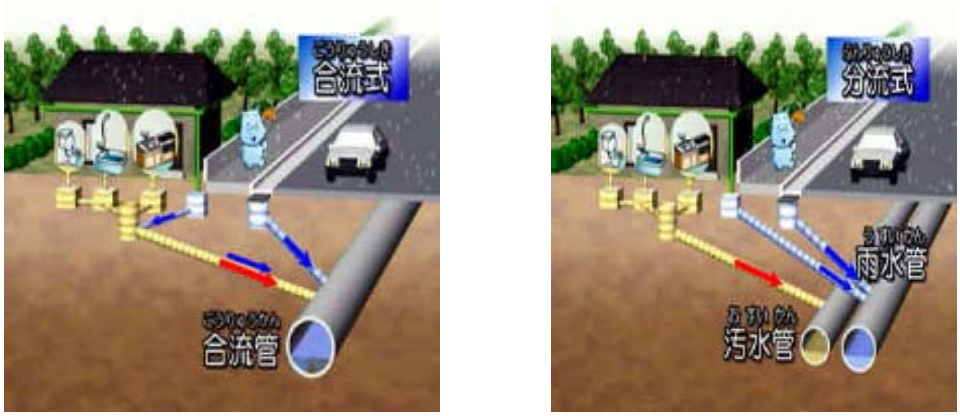

Fig. 1.1 combined (left) and separated (right) type of sewerage pipe (Onozawa, 2005)

The CSO outfalls to the waterway act as relief points for the excess flow in the sewers, thereby reducing the frequency and severity of sewer backups and flooding.

1.3 Impact of CSO

Many people visit to sea shore for recreation and consume sea foods. But the water bodies like Tokyo Bay that receive CSO contain pathogens which may cause many human diseases. Recreational Water Illness (RWI), caused by exposure to pathogens in surface waters, is a major public health concern. Common RWIs in the United States include diarrhea, respiratory, skin, ear and eye infections and other illnesses (CDC, 2004). It may also cause temporary water quality degradation in the waterways.

Concerns over RWIs lead to a significant number of beach closings all over the world. In 2002, 25% of surveyed beaches had at least one advisory or area closed, mostly (75%) due to elevated bacteria (USEPA, 2003). About 13% of streams and 17% of estuaries are considered impaired because of pathogens (USEPA, 2004).

Many locations, including the lower Charles River in Boston are permanently closed to swimming (Hellweger and Masopust, 2008). Swimming, surfing or other activities should be avoided and is not recommended, particularly during and immediately after rainfall.

1.4 Status of Tokyo sewerage system

The Kanda district sewer was the first Japanese modernized sewerage system constructed more than a century ago. A 100% sewerage system development for the Tokyo wards area reached in 1995. Scales of sewerage system are total length of sewers by 15,000 km, numbers of pumping stations by 78 and numbers of wastewater treatment plants by 14 (Sugita *et. al.,* 2003).

The total daily discharge of the huge STPs in the Tokyo metropolitan area (Fig. 1.2) amounts to more than 4 million m^3, which is comparable to the total water volume from some of the main rivers flowing into Tokyo Bay (Bureau of Sewerage, TMG, 2005).

Some of the wards have large lowland areas posing a high risk of flooding, and in the development of this vast sewer system great emphasis was laid on flood protection measures in concern with wastewater disposal. In view of this, the combined sewer system, which collects both wastewater and storm water, was adopted. As a result, most of the sewer system now consists of combined sewers, while the separate sewer, which is reputedly superior to the combined sewer in terms of pollution prevention, accounts for only 18% (Sugita *et. al.,* 2003).

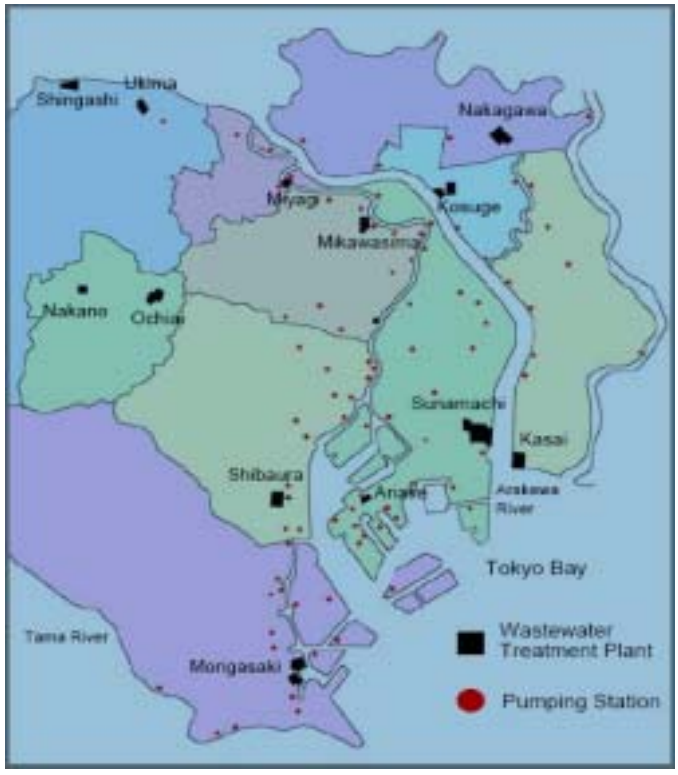

Fig. 1.2 Tokyo waste water treatment plant and pumping stations

There are approximately 800 points releasing combined sewerage overflow (CSO) in the Tokyo metropolitan area, with some of the major outfalls causing 30 to 50 CSO events every year around Tokyo Bay (Bureau of Sewerage, TMG, 2005).

1.5 Background and purpose of the study

Though the sewerage system of Tokyo metropolitan is well established, water quality degradation of Tokyo Bay is still taking place. The reason behind this is the overflowed sewer during storms (Fig.1.3). This overflowed sewage contains pathogens that are unhygienic for beach swimmers. To decrease the risk from introduced pathogens, monitoring that is both well designed and routine is essential.

Fig.1.3. CSO event due to heavy rain and beach of Odaiba, Tokyo Bay (Onozawa, 2005)

Although studies have examined the influences of storm water and CSO in terms of the release of microbial pathogens and anthropogenic compounds into Tokyo Bay, routine water quality monitoring has been conducted only under clear weather conditions. Therefore, little is known about the influences of storm water or CSO on the aquatic environment of Tokyo Bay. Moreover, it is difficult to accurately estimate CSO and the consequent flux of the pollution load into Tokyo Bay, because there is no system in place to measure water levels and flow rates of overflowed sewers during transient storm events (Maki, *et. al.*, 2007).

In addition, the physical environments of urban coastal zones vary widely depending on time and location. Their complicated geographical features border both inland and outer oceans, and so both inland and outer oceans affect them. For example, tidal currents, this is a dominant phenomenon in this area, oscillate according to diurnal periods. Even if the emitted levels of pathogens were constant and we could monitor the levels of pathogen indicator organisms at the same place, they would fluctuate according to tidal periods. Density stratification also changes with the tides (Onozawa *et. al.,* 2005).

A surprising number of pathogens have been reported in the sea, measuring these pathogens is difficult and time consuming — not least because such pathogens typically exist in a "viable but non-culturable" (VBNC) state. Consequently, the frequent measurement of pathogens is needed to discuss the risk pathogens pose in urban coastal zones. However, this kind of frequent monitoring appears to be impossible (Onozawa *et. al.,* 2005).

Current laboratory methods for monitoring bacterial indicators require at least 24 h of incubation, which results in delayed results (Hellweger and Masopust, 2008).

Moreover, some recent studies (Boehm *et. al*., 2002; Olyphantand Whitman, 2004) showed that there is a poor correlation between pathogen concentration on the sampling date and the next day when the results are available. The studies demonstrated the utility of modeling for estimating pathogen indicators. They also showed that concentration of the indicator organisms is typically a function of dynamic interacting processes. These processes operate at time and space scales not resolved by typical monitoring programs. So modeling can be a good alternative to solely monitoring.

To conclusively establish the ability of numerical modeling to represent the complex dynamic processes, the models should be tested at the spatial and temporal scale of the processes. In other words, observations that resolve plumes and peaks in space and time are needed.

Recent studies have shown that the fecal indicator bacteria (FIB) currently used to indicate coastal recreational water quality throughout the world may be inadequate to reflect human viral contamination (Jiang *et. al*., 2007). Coliform standards often fail to predict the occurrence of many waterborne human pathogens, such as pathogenic bacteria, the protozoan parasites *Cryptosporidium* and *Giardia*, and enteric viruses, which are most often the cause of disease from recreational exposure. Furthermore, traditional bacterial indicators generally die off quickly in marine water compared to viruses and protozoa (Fong *et. al*., 2004). Therefore, viruses are suspected to be important causative agents of waterborne illness along with coliforms.

Enteric viruses are more resistant than many other sewage-associated pathogens and bacterial indicators to extreme environmental conditions and conventional wastewater treatment, such as chlorination, UV radiation, and filtration (Thurston-Enriquez *et. al*., 2003). These viruses can also remain infective for long periods in the environment and have been reported to survive for up to 130 days in seawater, up to 120 days in sewage, and up to 100 days in soil at 20 to 30°C (Bosch *et. al*., 1995; Wetz *et. al*., 2004). These survival periods surpass those reported for fecal coliform and other indicator bacteria in similar environments (Fong *et. al*., 2005).

Moreover, human adenoviruses are the only human enteric viruses that contain double-stranded DNA instead of RNA, potentially are more stable in various environments, and are more resistant to UV irradiation and other water purification treatments than other human enteric viruses, because they are able to use the host cell DNA repair mechanism to repair damage in their DNA caused by UV irradiation (Gerba *et. al*., 2002). Therefore, the traditional bacterial indicators are not adequate to reflect the presence of pathogenic viruses.

Present study presents a case study in the inner Tokyo Bay to explain CSO events using *E. coli* and Adenovirus (AdV) as an indicator. The goal of the research was to determine and understand the important dynamic processes and modeling approach to support public health risk management (i.e. beach closing) for sailors, sea surfers and beach swimmers.

To achieve the goal, a three-dimensional hydrodynamic and water quality model coupled with a pathogen model at comparable resolution was applied. Field observations were also conducted to monitor the influences of storm water and CSO and to validate the numerical modeling.

1.6 Objectives

The objective of the study is to assess the influence of rainfall and CSO on Tokyo Bay by analyzing storm water which carries uncontrolled risk factor/agent at Tokyo Bay.

The specific objectives of this study are as follows:

- To understand the dynamics and distribution (timing & extent) of CSO responsible for water quality degradation by numerical simulation using *E. coli* and Adenovirus as an indicator.
- To determine the conditions (tide, wind, amount of rainfall) that are dominant factor for variations of water quality component.
- To find the appropriate CSO control technique for Tokyo Bay and provide a guideline (i.e safe time and location) for the sea surfers and swimmers.

2. LITERATURE REVIEW

2.1 Overview of coastal zone pollution

In recent years there has been an increased public awareness and concern regarding the pollution of coastal and inland waters, particularly where the waters have become increasingly used as receiving waters for the discharge of domestic effluents, industrial by-products, agricultural run-off and urban drainage (Harris *et. al*., 2004).

Oceans adjacent to large urban areas, or "urban oceans", are the final repositories of pollutants from a myriad of point and nonpoint sources of human waste. In spite of continuing improvements in control of point-source pollution, the water quality goals and designated uses of the receiving waters are unattainable without some advanced control of non-point-source (NPS) pollution. In urban areas, the most significant source of NPS pollution is urban runoff, which may reach the receiving waters either as discharges of storm water (SW) from storm sewers, or as combined sewer overflows (CSOs) (Marsalek, 2004).

A broad spectrum of contaminants is discharged into the coastal zone via direct discharge of sewage effluents or rivers receiving sewage. Sewage is known to be a major contributor of pollutants to coastal waters, so gaining an understanding of the spatial distribution and fate of sewage-derived contaminants in coastal zones is essential to manage the coastal environment (Managaki *et. al*., 2006). Wet-weather pollution can impact on receiving waters in many ways, the most difficult to control appears to be microbiological pollution, particularly in the case of CSOs (Marsalek, 2004).

2.2 Pathogen as an indicator of coastal zone pollution

Fecal coliform bacteria and other bacterial indicators have been used by most water quality regulators in the United States for over a century as standard tools to measure fecal contamination (Fong *et. al*., 2005). Coastal recreational water quality standards in California and throughout most of the world are based on the concentration of coliforms or *Enterococcus* spp., known as fecal indicator bacteria (FIB) (Jiang *et. al*., 2007). The discharge of viral pathogens in treated sewage is not regulated, and monitoring relies on bacterial indicator detection to predict virus contamination (Griffin *et. al*., 2003). However, the adequacy of current water quality standards to indicate the presence of

human viral pathogens is still questionable and it is now recognized that the absence or low concentrations of FIB in water may not adequately reflect the absence of human viruses (Jiang *et. al*., 2007).

Viruses are suspected to be important causative agents of waterborne illness; however, viral diseases are hard to identify by current diagnostic techniques. It was estimated that viral infection may be the causative agent of nearly 50% of all acute gastrointestinal illnesses. Therefore, viral contamination of recreational coastal water is of particular importance and is a rising public health concern (Jiang *et. al*., 2007).

Over 100 types of pathogenic viruses have been found in sewage-contaminated aquatic environments. These viruses, collectively known as enteric viruses, are transmitted via the fecal-oral route, and they infect and replicate in the gastrointestinal tract of the hosts. Enteric viruses are excreted in high concentrations in human and animal feces and, in certain cases, urine (Fong *et. al*., 2005). Enteric virus concentrations in raw sewage and polluted surface water have been estimated at around 10^2 viral particles 100 ml^{-1} and 1 to 10 viral particles 100 ml^{-1} respectively (Straub and Chandler, 2003). According to Griffin *et. al*., 2003, virus levels in wastewater range from 1.82×10^2 to 9.2×10^4 liter $^{-1}$ in untreated sewage and from 1.0×10^3 to 1.0×10^2 liter $^{-1}$ in treated wastewater depending on the level of treatment.

Adenovirus can be a significant indicator to monitor recreational water quality are commonly found in wastewater-impacted marine environments can cause a wide range of disease types, including respiratory, ocular, and gastrointestinal infections (Griffin *et. al*., 2003). Recent studies conducted in Europe have also suggested using adenoviruses as an index of pollution of human origin in waters, given their high numbers in sewage and contaminated aquatic environments and their unusual stability to chemical or physical agents and adverse pH conditions, allowing for prolonged survival outside of the body and water (Fong *et. al*., 2005). Adenoviruses have been found to survive three to five times longer than poliovirus in seawater, wastewater, and tap water (Enriquez *et. al.,* 1995).

Numerous epidemiological studies have found swimmers to be at increased risk of disease after swimming at polluted beaches. In Hong Kong it was estimated that swimmers were 2 to 20 times more likely to exhibit eye, skin, and respiratory symptoms than non swimmers (Kueh *et. al*., 1995). At a beach in Rams gate, United Kingdom, 24% of 1883 individuals reported at least one symptom of illness after swimming or

surfing at the beach and the relative risk was significant for bathers versus non bathers (Balarajan *et. al*., 1991). A competitive race, Swim around Key West, Florida, US was held in 1999. Surveys obtained from 160 swimmers who participated in the event reported that 31% had a least one symptom of disease following the event (Nobles *et. al.,* 2000),

The contamination of marine waters with viruses has been, and will continue to be, an important public health issue. The spread of viral diseases through recreational water exposure and ingestion of contaminated shellfish is a primary public health concern. The key to understanding and controlling viral contamination of our coastal environments is the application of new tools for monitoring and studying these microorganisms (Griffin *et. al*., 2003).

2.3 Studies related to pathogen level and distribution in coastal water

Barbé *et. al*. (2001) tested for correlation between fecal coliform and parameters such as rainfall up to four days prior to the fecal coliform measurement, salinity, water temperature and average daily wind speed in a shoreline study on the south shore of Lake Pontchartrain, Louisiana, US. Fecal coliform concentrations were found to be wet weather dependent. The study identified that fecal coliform levels were found to increase only after a pumping event. It was also found that the fecal coliform levels were a function of both rainfall amounts and salinity levels; a direct relationship exists between fecal coliform levels and precipitation while an inverse relationship exists between fecal coliform and salinity.

Lipp *et. al*. (2001) studied microbial pollution In Charlotte Harbor, Fla., found that an increase in rainfall and river discharge due to the 1997 to 1998 El Nin˜o season decreased estuarine salinity and increased the probability of detecting viable enteroviruses.

A 3-year study of French coastal waters indicated that the presence of viruses (enteroviruses, Human Adenovirus, Norwalk-like virus, astrovirus and rotavirus) in shellfish usually coincided with incidence of human disease and episodes of rain. These authors hypothesized that short, heavy winter rains caused an overload of sewage treatment facilities, resulting in contamination of shellfish beds (Miossec *et. al*., 2000). Whether the source of feces in a given region is due to indigenous wildlife or human

populations, precipitation events have been shown to significantly influence microbial water quality by increasing the bioload (Griffin *et. al*., 2003).

Hellweger and Masopust, 2008 observed a spatial and temporal patterns of E. coli in the lower Charles River, Boston, USA. They used a mechanistic coupled hydrodynamic and water quality model revealed that concentration of E-coli exhibits significant spatial and temporal structure at scales not resolved by monitoring programs. Therefore, the system should not be characterized as well-mixed and there is not a consistent relationship between rainfall or input and elevated E. coli concentrations. Outfalls may discharge rapidly and consistently after major storms, but the transport of the plume to another location may be longer and more variable, depending on instream hydrodynamic conditions. They also found that the Stony Brook and Muddy River are the predominant source of E. coli to the basin and that the spatial and temporal patterns are primarily driven by the hydrodynamics caused by operation of the New Charles River Dam and wind conditions, and die-off.

In a similar manner, Liu *et. al.* (2006) used a model to demonstrate that the water quality at a beach located between two pollutant sources can be influenced by either source, depending on the current direction. McCorquodale *et. al.* (2005) also used a model to demonstrate that instream transport can change significantly depending on the hydrodynamic conditions.

2.4 Review of some coastal ocean model

In connection with the consequential concerns relating to combating coastal pollution, there are now a range of hydroenvironmetal challenges which are increasingly being addressed world-wide. These challenges have resulted in a marked increase in the emphasis being placed on the research, development and application of numerical (or computer) models to predict complex flow fields and water quality indicator distributions in coastal and estuarine waters.

The rapid advances in computer hardware and software, particularly over the past two decades, have increased significantly the utilization of hydroenvironmetal models for environmental impact assessment studies. In comparison with physical models, numerical models involve modeling flow and pollutant transport processes at the prototype scale, and are generally considerably less expensive and more flexible, adaptable and portable. However, numerical models have disadvantages too. They involve the solution of complex differential equations governing the conservation of mass and momentum and the advection and diffusion of pollutants. The true solution of the flow and pollutant transport processes depends upon how accurately the solution of the equations and the equations themselves, reflect the actual flow and bio-chemical processes within the coastal or estuarine basin. Uncertainties encompassed within such models include: the fluid mechanics, e.g. turbulence; the physical processes, e.g. erosion and deposition of cohesive sediments; the chemical and biological processes relating to water quality parameters, e.g. decay rates for fecal coliforms; the numerical methods, e.g. the treatment of mathematical discontinuities; and the inclusion of boundary conditions, e.g. bathymetric data, currents, water levels, bed roughness lengths, etc. (Harris *et. al*., 2004).

Estuarine, Coastal and Ocean Modeling System with Sediments (ECOMSED):

ECOMSED is a three-dimensional hydrodynamic and sediment transport model developed by Blumberg and Mellor 1987. It includes separate modules for the computation of hydrodynamics, wind induced waves, sediment transport, transport of salinity, temperature, conservative and non conservative tracer, heat flux calculations, and particle tracking. ECOMSED allows the use of orthogonal curvilinear grids in the horizontal direction and is based on the sigma coordinate system in the vertical, making it suitable for coastal applications. However, the standard release version of ECOMSED does not allow simulating the wetting and drying of the grid cells in intertidal marshes and tidal flats. The model formulation uses the finite control volume principle.

The model has a two time step solution scheme. The horizontal (external) free surface mode solves the depth-average surface wave equation using a small time step. The internal mode solves the three-dimensional part using a much larger time step of the order of 40 times the external time step. It is a three time level model and time stepping is accomplished by the leap frog scheme.

Sediment module of ECOMSED allows to model cohesive and non-cohesive sediment transport including the combined effect of currents and waves. This makes ECOMSED ideal to model fate and transport of pathogens including the contribution of fecal coliform from the sediment.

ECOMSED have been used in number of sediment transport studies. Lick *et. al.* (1994) used ECOMSED to simulate the resuspension and transport of fine-grained sediments in Lake Erie for a variety of wind conditions. The study found that major storms, despite of their infrequent occurrence, contribute for most of the resuspension and transport of fine-grained sediments in Lake Erie.

Both the near field and far field behavior of the Sand Island, Hawaii, and ocean outfall plume were modeled by Connolly *et. al.* (1999). The three-dimensional circulation and water quality model was applied to predict the fate of pathogenic organisms in the vicinity of the outfall. Two nested numerical grids were generated for this application: one for the circulation model that extended around the island, and a grid for the fate and transport model that was more local in extent. The more extensive circulation model grid was needed in order to correctly simulate the observed circulation patterns in Mamala Bay. A conclusion of the study was that the Sand Island discharge was a primary contributor of observed fecal coliform levels on eastern recreational beaches. Other sources were identified as important for other beaches, and during storm events. The contribution of sediment as a fecal coliform source was neglected in this study.

2.5 Overview of the Present Numerical Model

Governing equations and boundary conditions:

All numerical ocean models solve one form or the other of the same equations for oceanic motions, written in the coordinate frame of reference fixed to the rotating earth. These equations are essentially Navier-Stokes equations with gravitational buoyancy force (Archimedian force due to density stratification) and Coriolis force (from fictitious accelerations generated due to the noninertial nature of the rotating coordinate frame) prominent in the dynamical balance (Kantha and Clayson, 2000).

In addition to this an equation of state relating to the density of seawater to its temperature and salinity (and pressure) and conservation equations for temperature and salinity are solved. When simulations for chemical or biological components are desired, conservation equations for the corresponding species are to be solved, with appropriate source and sink terms (Asad, 2006).

The equation expressing the conservation of momentum can be written in tensor

notation as;

$$\rho\frac{\partial u_i}{\partial t}+\rho u_j\frac{\partial u_i}{\partial x_j}+2\rho\varepsilon_{ijk}\Omega_j u_k=-\frac{\partial p}{\partial x_i}-g\rho\delta_{3j}+\frac{\partial \sigma_{ij}}{\partial x_j} \qquad (2.1)$$

Here ρ is density of water, *t* is time, *p* pressure, Ω*j* is the component of the Earth's angular velocity and σ_{ij} are the components of stress due to molecular viscosity.ε*ijk* = +1, if *i, j, k* are in cyclic order andε*ijk* = -1, if *i, j, k* are in anti-cyclic order and ε*ijk* = 0, if any pair or all three indices have the same value; $\delta_3 i$ =1 when *i* = 3 and δ3 *i* = 0 for otherwise.

Also, when μ is the molecular viscosity, the stress tensor σ*ij* , can be expressed in terms of the rate of deformation of the fluid element by motion.

$$\sigma_{ij}=\mu\left(\frac{\partial \mu_i}{\partial x_j}+\frac{\partial u_j}{\partial x_i}\right) \qquad (2.2)$$

An expansion into three equations can be made to obtain Navier-Stokes equation on fplane, upon which the present model is based which are as follows:

$$\frac{\partial u}{\partial t}+u\frac{\partial u}{\partial x}+v\frac{\partial u}{\partial y}+w\frac{\partial u}{\partial z}=fv-\frac{1}{\rho}\frac{\partial p}{\partial x}+\frac{\partial}{\partial x}(A_x\frac{\partial u}{\partial x})+\frac{\partial}{\partial y}(A_y\frac{\partial u}{\partial y})+\frac{\partial}{\partial z}(A_z\frac{\partial u}{\partial z}) \quad (2.3)$$

$$\frac{\partial v}{\partial t}+u\frac{\partial v}{\partial x}+v\frac{\partial v}{\partial y}+w\frac{\partial v}{\partial z}=fu-\frac{1}{\rho}\frac{\partial p}{\partial y}+\frac{\partial}{\partial x}(A_x\frac{\partial v}{\partial x})+\frac{\partial}{\partial y}(A_y\frac{\partial v}{\partial y})+\frac{\partial}{\partial z}(A_z\frac{\partial v}{\partial z}) \quad (2.3)$$

$$\frac{\partial w}{\partial t}+u\frac{\partial w}{\partial x}+v\frac{\partial w}{\partial y}+w\frac{\partial w}{\partial z}=-g-\frac{1}{\rho}\frac{\partial p}{\partial z}+\frac{\partial}{\partial x}(A_x\frac{\partial w}{\partial x})+\frac{\partial}{\partial y}(A_y\frac{\partial w}{\partial y})+\frac{\partial}{\partial z}(A_z\frac{\partial w}{\partial z}) \quad (2.4)$$

The conservation of mass can be expressed through the continuity equation

$$\frac{\partial \rho}{\partial t}+\frac{\partial \rho u_i}{\partial x_i}=0 \quad (2.5)$$

Which for an incompressible fluid become

$$\frac{\partial u_i}{\partial x_i}=0 \quad (2.6)$$

In expanded form the equation of mass-conservation;

$$\frac{\partial u}{\partial x}+\frac{\partial v}{\partial y}+\frac{\partial w}{\partial z}=0 \quad (2.7)$$

From hydrostatic pressure approximation,

$$\frac{\partial P}{\partial z}=-\rho g \quad (2.8)$$

Integrating between z to η

$$P(\eta)-P(z)=-\int_z^{\eta}\rho g \quad (2.9)$$

As, at surface P(η) = 0, is the constant reference density and ρ ' is the deviation from it

Equation (2.9) becomes:

$$-P(z) = -g\int_{Z}^{\eta}(\rho_0 + \rho')dz$$

$$P(z) = \rho_0 g(\eta - z) + g\int_{Z}^{\eta}\rho' dz \qquad (2.10)$$

$$\left[P_0 = \rho_0 g(\eta - z), P' = g\int_{Z}^{\eta}\rho' dz\right]$$

In equation (2.3), Boussinesq approximation is used whereby density is held constant except in the hydrostatic equation.

$$\frac{1}{\rho}\frac{\partial p}{\partial x} = \frac{1}{\rho}\frac{\partial}{\partial x}(P_0 + P')$$

$$\frac{1}{\rho}\frac{\partial p}{\partial x} = \frac{1}{\rho_0}\frac{\partial}{\partial x}\left[\rho_0 g(\eta - z) + g\int_{z}^{\eta}\rho' dz\right]$$

$$\frac{1}{\rho}\frac{\partial p}{\partial x} = g\frac{\partial}{\partial x}(\eta - z) + \frac{g}{\rho_0}\frac{\partial}{\partial x}\int_{z}^{\eta}\rho' dz$$

$$\frac{1}{\rho}\frac{\partial p}{\partial x} = g\frac{\partial \eta}{\partial x} + \frac{g}{\rho_0}\frac{\partial}{\partial x}\int_{z}^{\eta}\rho' dz$$

Similarly,

$$\frac{1}{\rho}\frac{\partial p}{\partial y} = g\frac{\partial \eta}{\partial y} + \frac{g}{\rho_0}\frac{\partial}{\partial y}\int_{z}^{\eta}\rho' dz$$

So the following two Boussinesq equations can be obtained from (2.3) and (2.4),

$$\frac{\partial u}{\partial t} + u\frac{\partial u}{\partial x} + v\frac{\partial u}{\partial y} + w\frac{\partial u}{\partial z} = fv - g\frac{\partial \eta}{\partial x} - \frac{g}{\rho_0}\frac{\partial}{\partial x}\int_{z}^{\eta}\rho' g dz + \frac{\partial}{\partial x}(A_x\frac{\partial u}{\partial x}) + \frac{\partial}{\partial y}(A_y\frac{\partial u}{\partial y}) + \frac{\partial}{\partial z}(A_z\frac{\partial u}{\partial z}) \qquad (2.11)$$

$$\frac{\partial v}{\partial t} + u\frac{\partial v}{\partial x} + v\frac{\partial v}{\partial y} + w\frac{\partial v}{\partial z} = fu - g\frac{\partial \eta}{\partial y} - \frac{g}{\rho_0}\frac{\partial}{\partial y}\int_{z}^{\eta}\rho' g dz + \frac{\partial}{\partial x}(A_x\frac{\partial v}{\partial x}) + \frac{\partial}{\partial y}(A_y\frac{\partial v}{\partial y}) + \frac{\partial}{\partial z}(A_z\frac{\partial v}{\partial z}) \qquad (2.12)$$

Conversion into sigma coordinate system:

$$\frac{\partial u}{\partial t}+u\frac{\partial u}{\partial x}+v\frac{\partial u}{\partial y}+w\frac{\partial u}{\partial z}$$

$$=\left|\frac{\partial u}{\partial t}\right|_{\sigma}+\frac{\partial u}{\partial \sigma}\left|\frac{\partial \sigma}{\partial t}\right|_{z}+u\left\{\left|\frac{\partial u}{\partial x}\right|_{\sigma}+\frac{\partial u}{\partial \sigma}\left|\frac{\partial \sigma}{\partial x}\right|_{z}\right\}+v\left\{\left|\frac{\partial u}{\partial y}\right|_{\sigma}+\frac{\partial u}{\partial \sigma}\left|\frac{\partial \sigma}{\partial y}\right|_{z}\right\}+w\frac{\partial \sigma}{\partial z}\frac{\partial u}{\partial \sigma}$$

$$Here, \dot{\sigma}=\frac{\partial \sigma}{\partial t}+u\frac{\partial \sigma}{\partial x}+v\frac{\partial \sigma}{\partial y}+w\frac{\partial \sigma}{\partial z}$$

$$\left|\frac{\partial u}{\partial t}+u\frac{\partial u}{\partial x}+v\frac{\partial u}{\partial y}+w\frac{\partial u}{\partial z}\right|_{z}=\left|\frac{\partial u}{\partial t}+u\frac{\partial u}{\partial x}+v\frac{\partial u}{\partial y}+\dot{\sigma}\frac{\partial u}{\partial \sigma}\right|_{\sigma} \quad (2.13)$$

Equation 3.11 is now:

$$H\left\{\frac{\partial u}{\partial t}+u\frac{\partial u}{\partial x}+v\frac{\partial u}{\partial y}+\dot{\sigma}\frac{\partial u}{\partial \sigma}\right\}+u\left\{\frac{\partial \eta}{\partial t}+\frac{\partial (Hu)}{\partial x}+\frac{\partial (Hv)}{\partial y}+\frac{\partial (H\dot{\sigma})}{\partial \dot{\sigma}}\right\}$$

$$=H\frac{\partial u}{\partial t}+Hu\frac{\partial u}{\partial x}+Hv\frac{\partial u}{\partial y}+H\dot{\sigma}\frac{\partial u}{\partial \sigma}+u\frac{\partial H}{\partial t}+u\frac{\partial (Hu)}{\partial x}+u\frac{\partial (Hv)}{\partial y}+u\frac{\partial (H\dot{\sigma})}{\partial \dot{\sigma}}$$

$$=\frac{\partial (Hu)}{\partial t}+\frac{\partial (Huu)}{\partial x}+\frac{\partial (Hvu)}{\partial y}+\frac{\partial (H\dot{\sigma}u)}{\partial \sigma} \quad (2.14)$$

$$Similarly, \frac{\partial (Hv)}{\partial t}+\frac{\partial (Huv)}{\partial x}+\frac{\partial (Hvv)}{\partial y}+\frac{\partial (H\dot{\sigma}v)}{\partial \sigma} \quad (2.15)$$

For the numerical solution of the above set of equations, traditionally two simplifying approximations are used.

(i) Hydrostatic approximation:

It exploits the fact that the aspect ratio of oceans is small and hence the vertical motions are small and also are further inhibited by gravitational forces under stable density stratification. This means vertical accelerations are small and the fluid acts as though it is under static equilibrium as far as vertical motion is concerned (Asad, 2006).

According to Prudman (1953), it is assumed that there is perfect balance between pressure gradient and gravity, in other words no acceleration in vertical direction.

(ii) Boussinesq approximation:

This approximation takes advantage of the fact that the density variations in the oceans are small (less than 3% or so) and therefore the density can be considered to be constant, except when body forces due to the motion of a density stratified fluid in a gravitational field are concerned. In other words, changes in the mass or inertia of a fluid parcel due to the changes in its density are negligible, while the same changes in density are consequential when gravitational field are present (Kantha and Clayson, 2000). So, following Boussinesq (1903), this approximation implies replacing ρ by a constant reference density ρ_0 everywhere except in terms involving gravitational acceleration constant g.

Implementation of these two approximations and conversion into sigma coordinate system leads to the following three governing equations where the first one (3.9) stands for mass conservation and the later two (3.10) for the conservation of momentum;

$$\frac{\partial \zeta}{\partial t}+\frac{\partial (uH)}{\partial x}+\frac{\partial (vH)}{\partial y}+\frac{\partial (\dot{\sigma} H)}{\partial \sigma}=0$$

$$\frac{\partial (H\tilde{\tilde{u}})}{\partial x}+\frac{\partial (H\tilde{\tilde{u}}u)}{\partial x}+\frac{\partial (H\tilde{\tilde{u}}v)}{\partial y}+\frac{\partial (H\tilde{\tilde{u}}\dot{\sigma})}{\partial \sigma}=Hf\begin{pmatrix} v \\ -u \end{pmatrix}-\frac{H}{\rho}\nabla P+HA_H\left(\frac{\delta^2\tilde{\tilde{u}}}{\delta x^2}+\frac{\delta^2\tilde{\tilde{u}}}{\delta y^2}\right)+\frac{1}{H}A_\sigma\frac{\delta^2\tilde{\tilde{u}}}{\delta \sigma^2}$$

Where; (2.16)

$$-\frac{\nabla P}{\rho}=-\frac{g}{\rho}(\rho_0+\sigma\rho')\nabla\zeta-\frac{\rho' g}{\rho}(\sigma-1)\nabla h-\frac{1}{\rho}\nabla\left(H\int_\sigma^1\rho' g d\sigma\right)$$

Boundary conditions:

Bottom friction is considered at bottom boundary condition:

$$A_\sigma \frac{\partial u}{\partial \sigma} = H \frac{\tau_x^b}{\rho} \quad (2.18)$$

$$A_\sigma \frac{\partial v}{\partial \sigma} = H \frac{\tau_y^b}{\rho} \quad (2.17)$$

Here,

$$\tau_x^b = \rho y_b^2 u \sqrt{u^2 + v^2}$$

$$\tau_y^b = \rho y_b^2 v \sqrt{u^2 + v^2}$$

Bottom friction coefficient y_b^2 is taken as 0.0026 (Sasaki and Isobe, 1996).

Wind-stress is considered at surface boundary condition:

$$A_\sigma \frac{\partial u}{\partial \sigma} = H \frac{\tau_x^s}{\rho} \quad (2.19)$$

$$A_\sigma \frac{\partial v}{\partial \sigma} = H \frac{\tau_y^s}{\rho} \quad (2.20)$$

Here,

$$\tau_x^s = \tau_s \cos\theta$$

$$\tau_y^s = \tau_s \sin\theta$$

$$\tau_s = \rho_a c_f U_{10}^2$$

Wind drag coefficient *f c* is considered constant, 0.0012.

At lateral boundaries, normal velocities are set as zero and a free slip condition is applied to the friction terms. At open boundary, velocity gradient is set as zero.

Vertical eddy viscosity and diffusivity are calculated from ‘zero equation’ mixing length model (MLM) from Kolmogorov’s hypothesis of similarity based on Richardson number and Monin-Obukhov’s similarity theory based on turbulent Prandtl number (Sasaki and Isobe, 1996). Constant values of horizontal viscosity and diffusivity are used.

A semi-implicit finite difference scheme is adopted where equations are discretized explicitly in the horizontal direction and implicitly in the vertical direction. Staggered Arakawa C grid is used with first order upwind scheme. The tri-diagonal formation of the momentum equation is utilized and in combination with the mass conservation equation, an algebraic equation is obtained where the only unknown is the surface elevation in implicit form. This algebraic equation is solved through successive over relaxation (SOR).

Governing equations for Temperature and Salinity:

The governing equations for temperature and salinity in sigma coordinate system:

$$\frac{\partial(HT)}{\partial t}+\frac{\partial(uHT)}{\partial x}+\frac{\partial(vHT)}{\partial y}+\frac{\partial(\dot{\sigma}HT)}{\partial \sigma}$$

$$=HK_H\left(\frac{\partial^2 T}{\partial x^2}+\frac{\partial^2 T}{\partial y^2}\right)+\frac{1}{H^2}\frac{\partial}{\partial \sigma}\left(K\nu\frac{\partial HT}{\partial \sigma}\right)+\frac{1}{\rho C_p}\frac{dq(\sigma)}{d\sigma} \quad (2.21)$$

$$\frac{\partial(HS)}{\partial t}+\frac{\partial(uHS)}{\partial x}+\frac{\partial(vHS)}{\partial y}+\frac{\partial(\dot{\sigma}HS)}{\partial \sigma}=HK_H\left(\frac{\partial^2 S}{\partial x^2}+\frac{\partial^2 S}{\partial y^2}\right)+\frac{1}{H^2}\frac{\partial}{\partial \sigma}\left(K\nu\frac{\partial HS}{\partial \sigma}\right)-RS \quad (2.22)$$

Boundary Conditions:

For conservation of temperature, sea surface boundary condition:

$$-\frac{1}{H^2}K\nu\frac{\partial(HT)}{\partial \sigma}=\frac{Q_s}{\rho C_p} \quad (2.23)$$

Net sea surface heat flux penetrating into the water column, *Qs* is expressed as follows;

$$Q_s=(1-A)Q_A-Q_B-Q_e-Q_h \quad (2.24)$$

Albedo (A) is set as 0.02

For conservation of salinity, sea surface boundary condition:

$$-\frac{1}{H^2}K\nu\frac{\partial(HS)}{\partial \sigma}=S(P-E_{rate}) \quad (2.25)$$

Here, *Erate* means evaporation rate.

Temperature and salinity equations (and also equations for other scalars) are discretized in the same manner as the momentum equations, vertical diffusion and vertical advection terms implicitly and other explicitly. The finite difference form shapes up a system of tri-diagonal system of equations and is solved efficiently through Tri-Diagonal Matrix Algorithm (TDMA).

2.6 CSO and its Control Mechanism

Urban runoff and CSOs are major contributors to water quality problems in coastal urban areas. Stormwater and CSO abatement requirements should be based to the greatest extent possible on an understanding of regional and local hydrology and coastal oceanography. They should be designed in conjunction with other regional environmental protection programs to produce the most cost-effective program for achieving the desired level of protection for receiving waters (NRC, 1993).

Many cities in Japan including Tokyo have combined collection systems that carry both stormwater and municipal sewage. During even small rainstorms, these systems can overflow, discharging untreated sewage, industrial wastewater, and urban runoff into nearby waterways.

The way in which urban runoff and CSOs affect receiving waters is significantly different from continuous point loadings. Rainfall induced loads are not constant, but intermittent, pulsed loads. In general the greatest concentrations of pollutants is contained in the first flash of stormwater, with concentrations decreasing as a storm continues. Reducing pollutant loads from unban runoff and CSOs is significantly more challenging and potentially more costly than removing pollutants from municipal and industrial wastewaters. Wastewater treatment processes are designed to treat relatively constant and continuous flows, and perform poorly when subjected to the extreme variations in flow that are characteristic of stormwater flows (NRC, 1993).

Currently, to mitigate CSO pollutions, the construction of storage tanks at 3 sites in Tokyo has been planned by the Tokyo Metropolitan Government. Shibaura is the target area of this plan around the Odaiba area. This plan for dealing with CSOs is not enough to mitigate the effects of CSOs completely. Again given the cost of constructing storage facilities on a large scale in urban areas, it is needed to deal with CSOs and to meet the environmental protection requirements of a particular region in a cost-effective way.

During wet weather, inflows may exceed the collection system's capacity and trigger a CSO. A typical CSO flow diagram is shown in the figure below (Fig. 2.1).

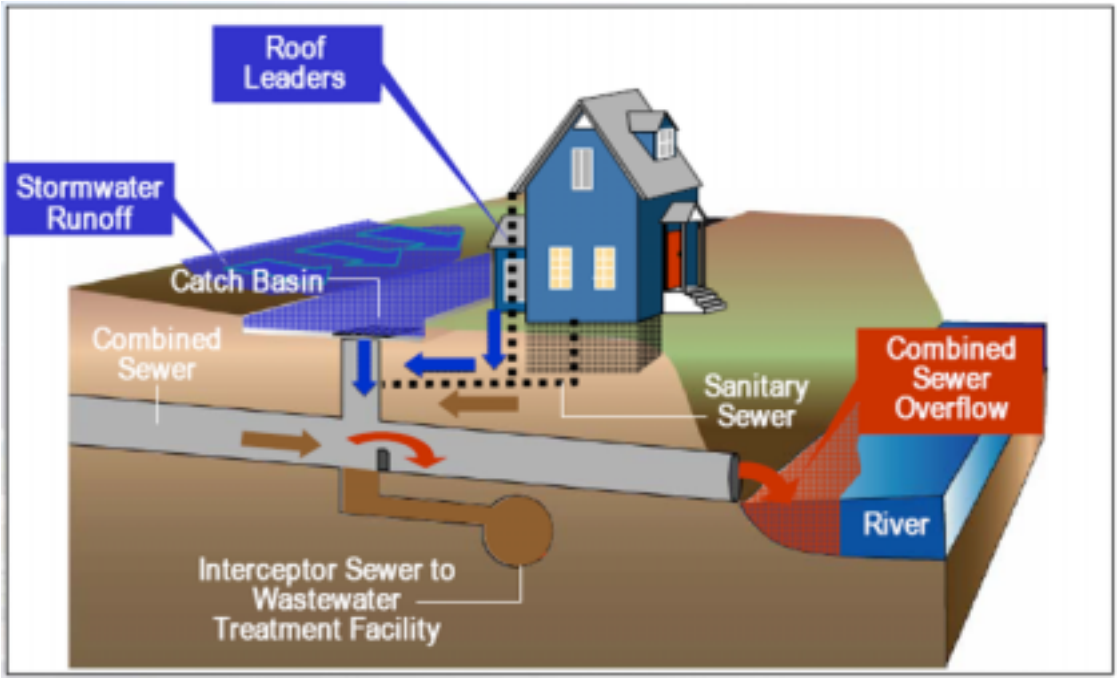

*Fig. 2.1 A typical CSO flowchart (*Fordiani, 2006)

There are different options to control CSOs.

1. Source controls,
2. Sewer system modification,
3. Sewer separation,
4. Storage facilities

Source controls:

It deals with reducing the amount of pollutants that accumulate during dry weather on the land surface, streets, and within sewer systems. Minimizing these accumulations means that during rainstorms there will be a smaller pollutant mass discharged from the urban land areas to receiving waters. Though, this is the cleanest and most obvious class of control, long term dependency on a labor force to perform these types of controls simply difficult.

Sewer system modification:

This system involves adjusting the flow controls within existing pipe systems to maximize the carrying capacity of interceptors (Fig. 2.2) or to take advantage of unused large pipe storage during wet weather. This system also includes flow redirection (Fig 2.3), diverting and reduce the flow to the system (Fig. 2.4). Inflow Reduction can be done by making detention ponds, inflow reduction by roof leader disconnection (Fig. 2.5), infiltration reduction, repair existing pipe and rehabilitate manholes.

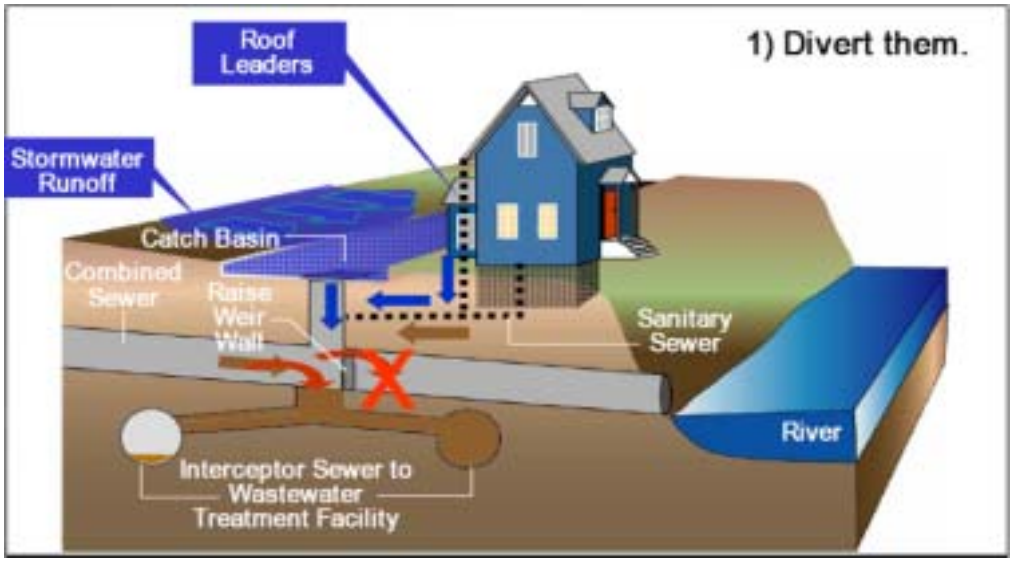

Fig.2.2. Preventing overflow by increasing interceptor sewer capacity (Fordiani, 2006)

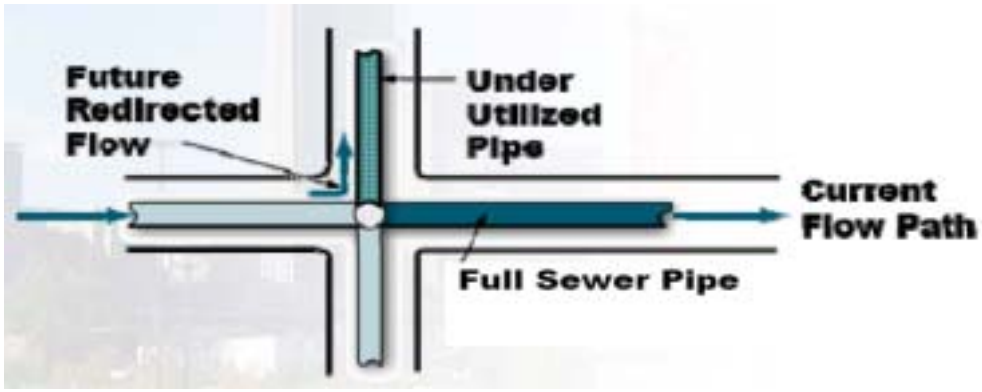

Fig.2.3. Preventing overflow by flow redirection (Fordiani, 2006)

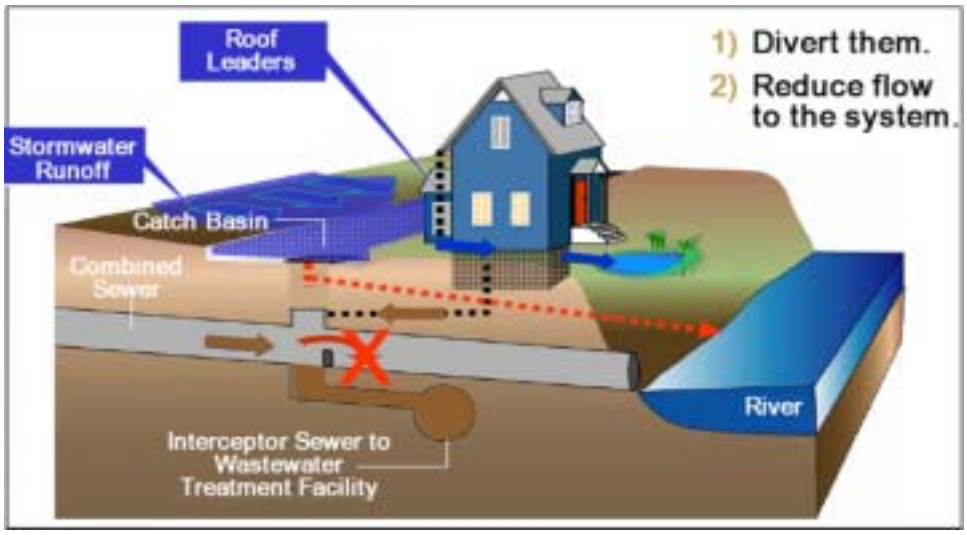

Fig.2.4. Preventing overflow by diverting and reducing flow to the system (Fordiani, 2006)

Fig.2.5. Roof leader disconnection to reduce flow to the system (Fordiani, 2006)

Sewer separation:

It is a method of minimizing the amount of street runoff that mixes with sanitary sewage. However, complete separation is difficult and prohibitively expensive to achieve. Existing combined sewer systems are likely more than 100 years old and under capacity for current development. It causes infrastructure replacement and community disruptions. Even separation done, but future treatment of storm water may be required. Now a day, this practice within combined-sewered areas is not practiced on a large scale. Separation is still practiced to solve pollution problems within small portions of combined sewer areas connected to separated systems or to solve flooding problems within combined systems where there is inadequate flow capacity. Figure 2.6 shows sewer separation system.

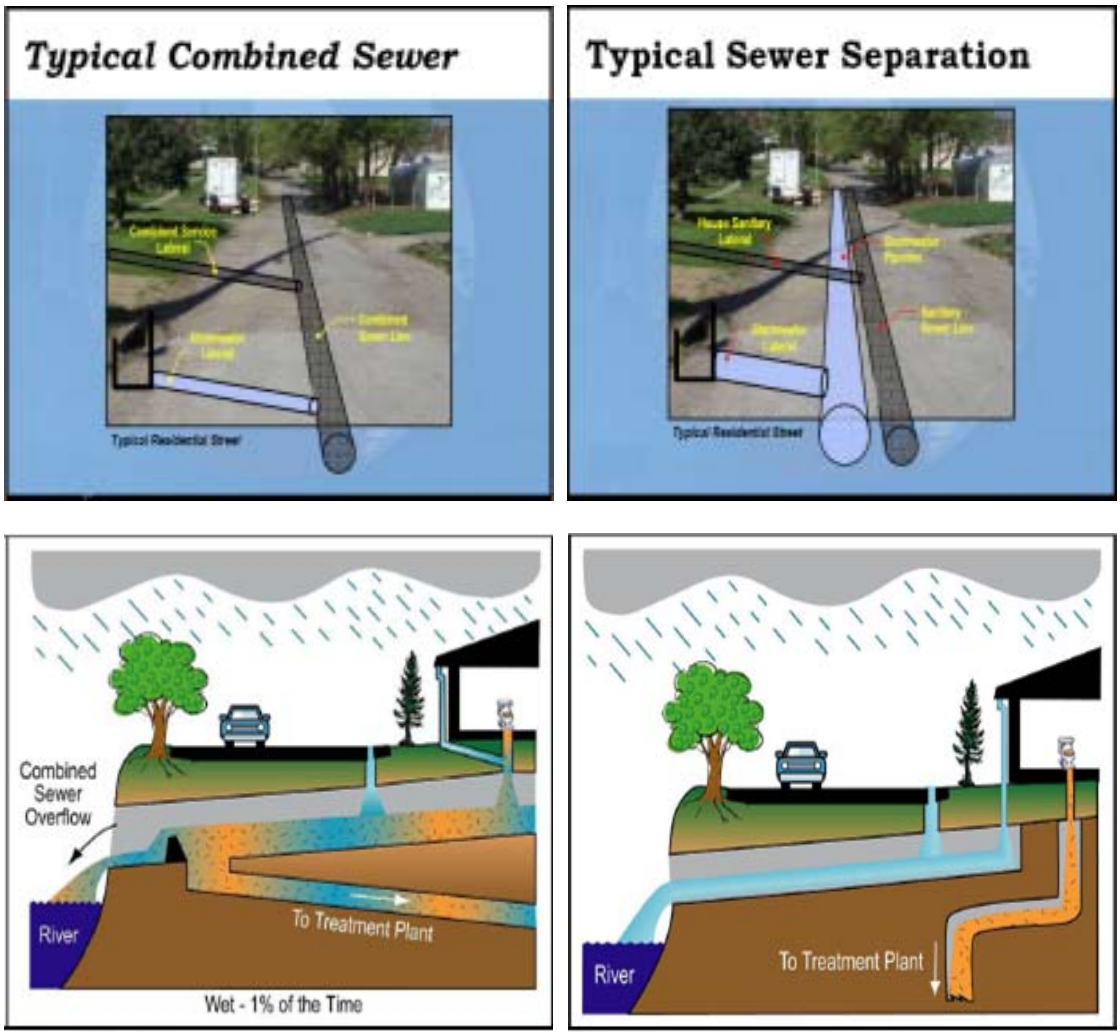

Fig.2.6. Sewer separation to reduce flow to the treatment plant (Fordiani, 2006)

Storage facilities:

Storage facilities, basins or tunnels have been extensively used to capture excess runoff during storm events. Storage allows the maximum use of existing dry weather treatment facilities and is often the best low cost solution to CSO problems. CSO is stored until the treatment facilities can treat the excess flows. Fig. 5.8 shows the position of a storage tank.

Two types of storage:

a) In-line Storage

It is provided in series with the existing sewer system as either construction of new tanks and/or oversized conduits to provide storage capacity. Tanks are designed to allow dry weather flows to pass through, while flows above the design peak is restricted, causing the tanks to fill.

b) Off-line storage

Constructed parallel to the existing system utilizing tanks, conduits, or underground tunnels having facilities for either draining by gravity or pumping flow to and from storage.

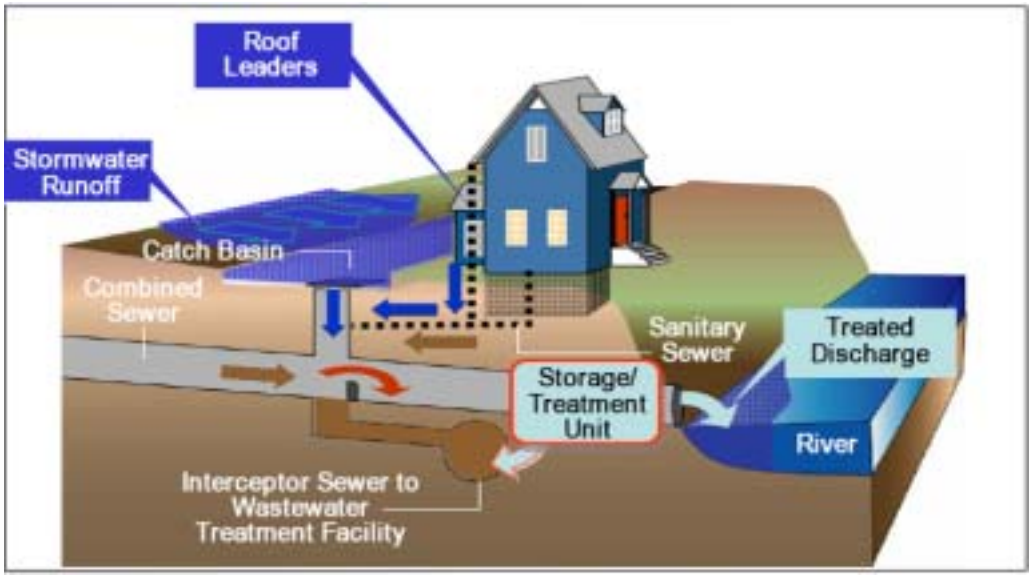

Fig. 2.7. Design of Storage treatment unit to store and treat CSOs (Fordiani, 2006)

CHAPTER 3: MATERIALS AND METHODS

3.1 Site description

The study site is the upper bay area (Odaiba) of Tokyo Bay (Fig. 3.1) which is located at the central part of main island (Honshu), Japan. The bay stretches 50 kilometers north to south, 20 kilometers east to west and its average depth is 18 m with the western side being deeper than the east. Its size (960 km2) is forth in Japan and nearly 20 percent of Japan's industrial and economic activity is concentrated around the area of this bay (Furukawa, 2003). This results in a severe population pressure of 26 million people living in the drainage basin of the bay. As a result, Tokyo Bay is a classic example of an estuary suffering profoundly due to urbanization and rapid development in its surrounding areas. The human as well as industrial activity around the bay area causes a huge amount pollutant and pathogen load into the bay.

Total twelve rivers discharge into Tokyo Bay with major discharge from Tama, Edo and Ara rivers all located along upper western area of the bay. According to the Japan Scientists Association 1979, annually, 10 km^3 of fresh water from rivers drains into the bay. The Edogawa River (3.4 km^3 of annual fresh water discharge), the Arakawa River (2.4 km^3), the Sumidagawa River (1.6 km^3) and the Tamagawa River (1.2 km^3) contribute about 90% of the fresh water that arrives in the bay. Hosokawa (2003) also mentioned that the annual inflow of fresh water into Tokyo Bay from its rivers is approximately 10^{10} cubic meter. Radjawane *et. al.* (2001) has mentioned that the monthly mean of the total volume of fresh water discharged into Tokyo Bay was 110m^3/s and it ranged from 75m^3/s to 250m^3/s during the days of August in 1995.

For the rivers entering Tokyo Bay the maximum discharge reaches during the rainy season in Kanto region (between July and August) and also during the typhoon season of September and October another high discharge is also expected (Asad, 2006).

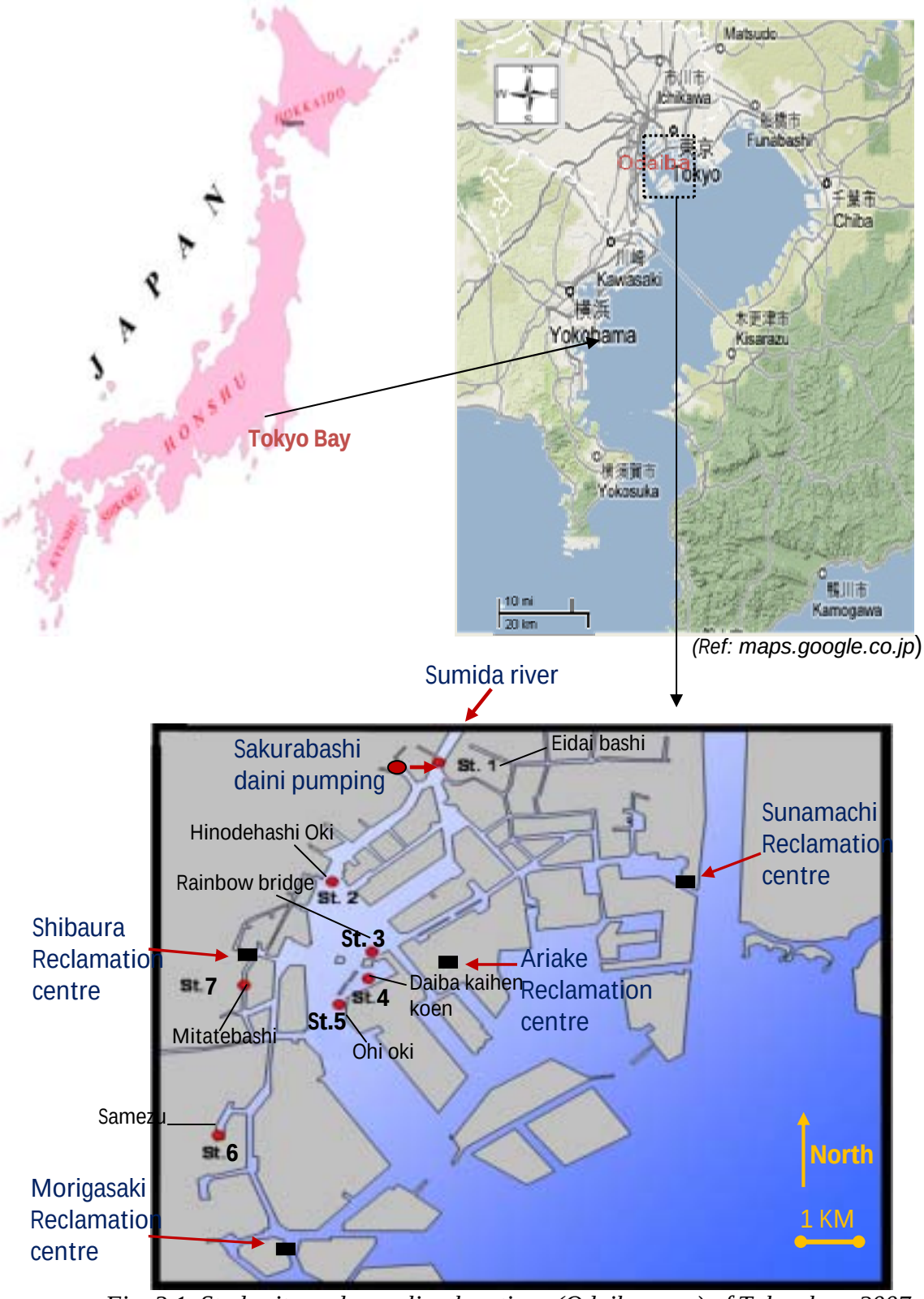

Fig. 3.1. Study site and sampling locations (Odaiba area) of Tokyo bay, 2007

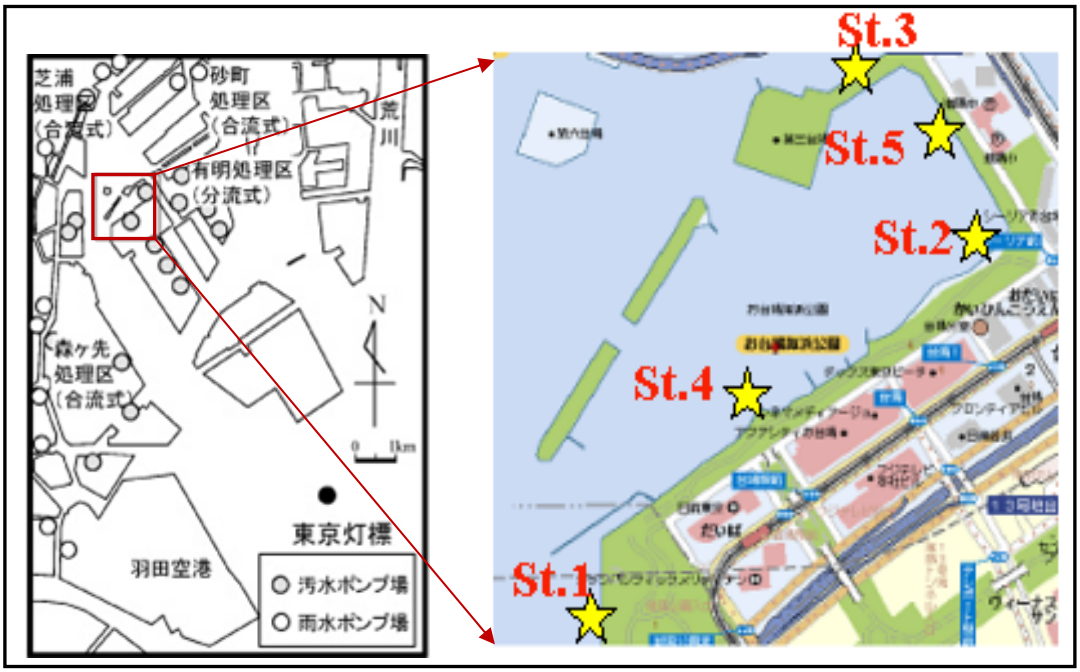

Fig. 3.2. Sampling locations (Odaiba area) of Tokyo Bay, 2004

3.2 Field sampling

The sampling locations in Odaiba area of Tokyo Bay are shown in Fig. 3.1. To characterize the rainfall effects on the levels of pathogen and water quality indicators 5 days sampling was done at November, 2007 (11^{th} 12^{th} 14^{th} 21^{th} 28^{th}) just after 26.5 mm rainfall on November 10^{th}. Sampling was done both at High tide and Low tide. The rainfall and tidal position during sampling time are shown in figure 3.3. Rainfall data was collected from Japan Meteorological Agency website (http://www.jma.go.jp) and the station is Otemachi located near Tokyo Bay. In order to know the vertical distribution of water quality parameters samples were taken from 3 layers (Surface, Middle and Bottom). Total 95 samples from 7 sampling stations were collected in order to know the following water quality parameters: health related bacteria's and viruses, nutrients (TN, NH_4-N, NO_2-N, NO_3-N, PO_4-P, TP), Suspended Solids, Total Organic carbon, Dissolved Organic Carbon, turbidity, salinity, temperature, Electric Conductivity, DO and pH. Numerical simulation was performed only at station 3, 4 and 5 due to lack of observed data.

Field observation was also conducted by Mr. Onozawa during his bachelor study in 2004 in the same site of Odaiba. He sampled in the 5 stations in Odaiba (see Fig. 3.2). Station 3, 2 and 1 is the same place of the present study stations of 3, 4 and 5. As observation stations 3, 2 and 1 in 2004 coincide with the observation stations 3, 4 and 5 of the present study, the data from those particular stations was used as a secondary data to validate the numerical modeling.

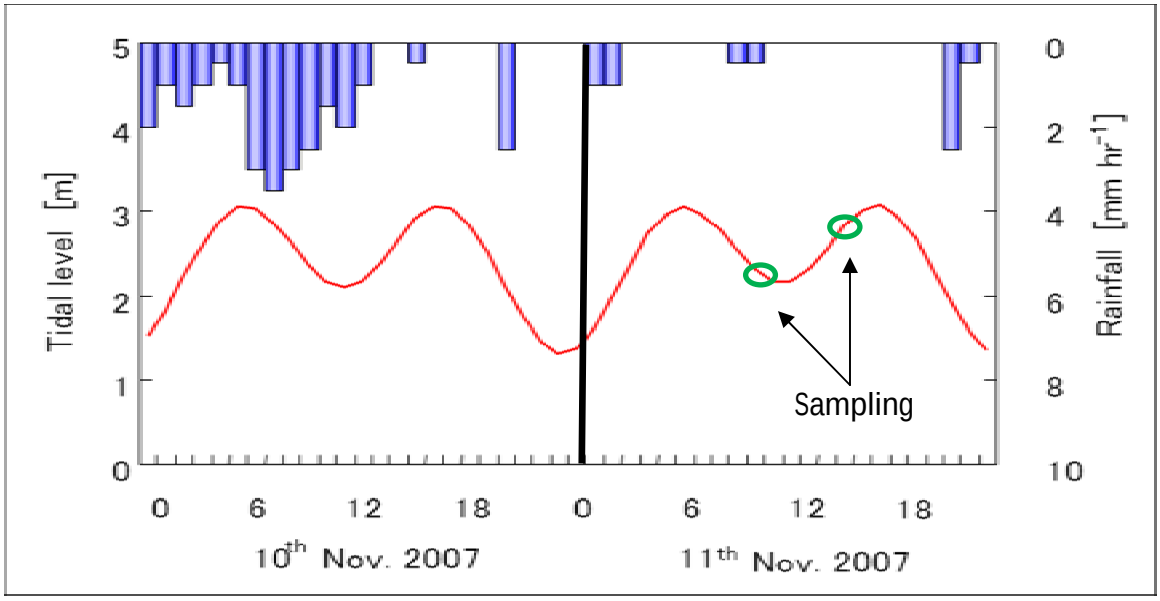

Fig. 3.3. The rainfall and tidal position during sampling at November 11, 2007

3.3 Analytical methods

Both In- Situ- Measurements in the field and Laboratory analysis (Fig. 3.4) was done. Water Depth (m), Water Temperature (^{0}C), Conductivity (µS/cm), Dissolved Oxygen (% and mg/L), pH, and Turbidity (NTU) were measured as an in-situ measurement in the defined stations using Alec Compact-CTW and sensors. Table 3.1 shows the types of instruments used for collecting different water quality parameters.

Samples were held on ice during sampling and transport to the laboratory. Afterward, they were kept in the cold room at 4^{0}C. For nutrient analysis membrane filtration was done except those sample that was used for TN and TP measurement.

For total nitrogen (TN), total phosphorus (TP), NH_4+-N, PO_4^{3-}-P, the Auto Analyzer 3-AACS- III (BRAN + LUEBBE) (Fig. 3.5) and Auto Sampler (BRAN + LUEBBE) were used and for digestion of the unfiltered sample to analyze the TN and TP, Autoclave SP 200F (YAMATO Scientific Co. LTD) was used. The analysis was carried after preparing the reagents and standard solutions as prescribed by the standard manual of the instrument (AACS III Analysis Method, 1999, BRAN+LUEBBE) and Standard Methods for the Examination of Water and Wastewater, APHA. The absorbance was measured at standard wave lengths such as NH_4^+-N at 630 nm, PO_4^{3-}-P at 880 nm, NO_3 –N and NO_2–N at 550 nm for specific nutrients to be analyzed. The correlation between the absorbance and concentration of the standard solutions gives the basis of measurement for the samples.

Window based BRATTEC Version 5.1 was used as software for the analysis and measurement processes.

Bacterial and viral (*E. coli*, *T. coli,* AdV) data were kindly provided by Furumai-lab, Department of Urban Engineering (Hongo campus), University of Tokyo. All the pathogen data are presented as colony-forming units (CFU) per 100 ml of water.

Table 3.1 Instruments for field measurement

Instrument	**Parameter**
Alec Compact-CTW	Salinity, Temperature
Multisensory (HORIBA U-10)	Turbidity, DO, EC, pH
TOC analyzer (SHIMAZDU TOC-V)	TOC, DOC, and TN
Potassium peroxydisulfate decomposition method	TP
AACS -III Auto Analyzer (BRAN+LUEBBE)	NH_4-N, NO_2-N, NO_3-N, PO_4-P

Fig. 3.4 Sampling and Laboratory analysis

Fig. 3.5. Nutrients Analysis AACS III (BRAN+LUBBEE)

3.4 Numerical Modeling

3.4.1 Model framework

The selection of the model that is apt for a given system is influenced by factors such as the scale and geometry of the system, the time scale of the processes, the driving forces in the system, and the physical processes occurring in the system. A brief review of the various models considered for this study was given in the Chapter 2.4. After the review, the present numerical model was selected considering its applicability to the coastal environments similar to Tokyo Bay. The model, first developed by Sasaki and Isobe (1996) and then later by Koibuchi and Isobe (2001).

This is a three-dimensional, time-variable, hydrodynamic model which solves equations for Navier-Stokes, conservation of mass, momentum, temperature, salinity, turbulence kinetic energy and turbulence macroscale. The governing equations and boundary conditions of this model are presented in the previous chapter (see chapter 2.5).

3.4.2 Model Input

In the present study by this model, the numerical simulations performed with two nested domains to fit the complex geographical feature around the Odaiba area (Fig. 3.6). The two computational domains cover the whole region of Tokyo Bay (50km × 66km) and the Odaiba area (5km × 12.7km) with grid resolutions of 2km and 100m, respectively. The first domain size is 25x33 grid points and the second domain has 50x127 grid points. All of the domains have 10 vertical sigma layers. A detailed configuration of the model is summarized in Table 3.2. These nested grids are able to represent vertical density gradients and hydrodynamics. The model period is from August 1, 2004, to October 15, 2004, total 76 days. The time step Δt = 10 mins for domain 1 and Δt = 30s for fine grid domain 2.

Table. 3.2. Boundary conditions and grid resolution

	Domain 1	**Domain 2**
Computational Area	50km×66km	5km×12.7km
Grid size	2000m	100m
Number of grid	25×33×10layer=8250	50×127×10layer=63500
Total number of Grid	2920	22740
Computational duration	2004/August/1~October/15	2004/August/1~October/15
Time step	10 minutes	30 seconds
Total time step	12660step	218800step

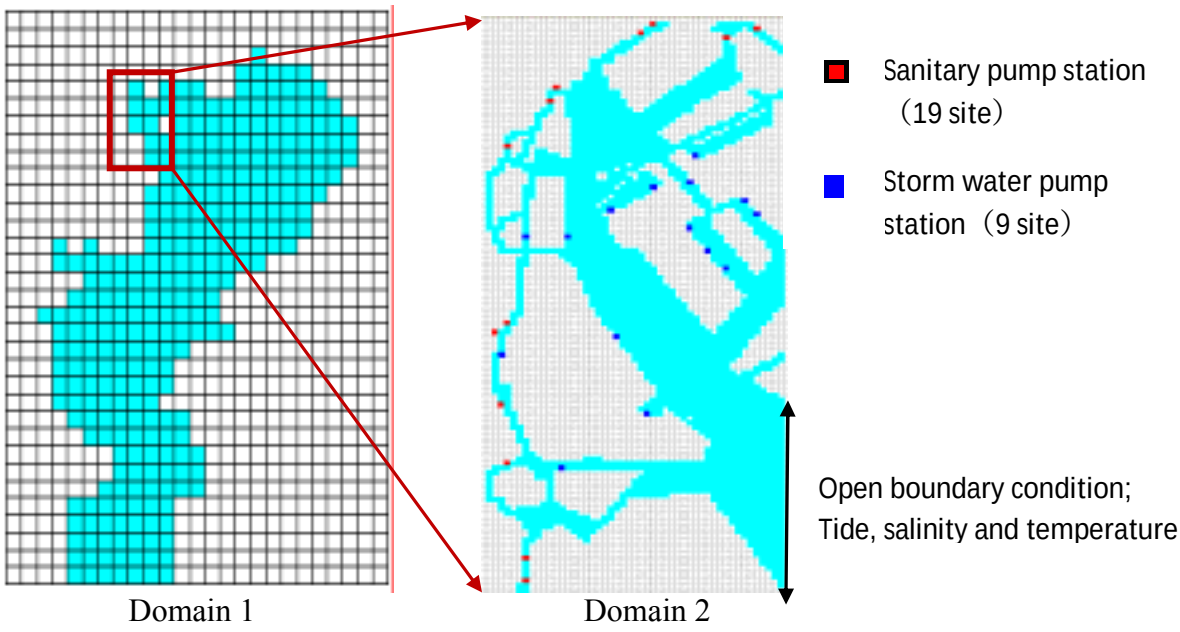

Fig. 3.6 Two nested computational domains. Left domain 1, whole bay area and right domain 2 with pumping station distributions around the Odaiba area

3.4.3 Pathogen model

The modeling of major pathogens of concern (including Enterovirus, Rotavirus, Norovirus, and Coronavirus) is not usually conducted due to the difficulty of modeling and the lack of observational data in the study area. We modeled *E. coli* and Adenovirus by using experimental data in the study site. The model discussed above has customized and coupled with a pathogen model (Onozawa *et. al.* 2005) to simulate *E. coli* and Adenovirus.

Modeling of Pathogen

Fecal bacteria are subject to a number of fate and transport processes. Fate processes include die-off, which depends on temperature, pH, nutrients, toxins, salinity and sunlight intensity, death by predation, as well as growth (cell division) and recovery of non-culturable cells. Transport processes include advection and dispersion, as well as settling to and resuspension from the sediment bed (Hellweger and Masopust, 2008).

The mathematical framework employed in the Pathogen model to reflect the fate and transport process of *E. coli* and AdV is expressed as follows:

$$\frac{\partial C}{\partial t} + u_i \frac{\partial C}{\partial x_i} + (-Sink)\frac{\partial C}{\partial z} = \frac{\partial}{\partial x_i}\left(\varepsilon_i \frac{\partial C}{\partial x_i}\right) - sal \cdot C$$

Where C denotes concentrations of Pathogen, *E. coli* or AdV (CFU/100ml), and t is time. *Sink* represents the sinking speed of Pathogen. u_i denotes flow speed for the calculation of the advection term. ε_i denotes the diffusion coefficients. *sal* denotes the

salinity-dependent die-off rate (/ppt-day). Here, the die-off due to decay process was included using a constant decay rate, 2.3 day^{-1} for *E. coli*. The survival rate of virus is higher than coliform. According to Gabriel, 2005, decay rate of AdV is 0.033/hr. So the equivalent rate of 0.792/day is used for Adv.

Sunlight is generally recognized to be one source by which bacteria are inactivated, due to UV damage to the bacterial cell (Sinton *et. al.* 2002). However, this particular target area has high turbidity that rapidly absorbs UV rays at the sea's surface. Hellweger and Masopust (2008) found that as the turbidity in the near-shore areas were higher, which would increase light extinction and counteract the effect of the shallower water column. They found that making *E. coli* die-off a function of sunlight intensity did not improve their model results. Liu *et. al*. (2006) also found that making die-off sunlight-dependent did not improve their model results. Again, Adv can tolerate much greater exposure to UV radiation than others, because they possess the cell repair mechanisms. As a result, sunlight-dependent die-off process has been ignored in this model.

The present pathogen model has been developed considering all the input and transport processes except resuspension from the bottom sediment. Pathogen concentration is related with particle resuspension which is as a function of wind speed. In shallow environments, under certain conditions of fetch, wind velocity, bathymetry and bottom characteristics, resuspension can be generated by wind induced waves. Winds with a speed >3 m s^{-1} allow particle resuspension which is effective for depths<1.5 m (Robert *et. al*., 1994).

Resuspension process depends mainly on wind speed and water depth. As the depth of the particular area (11-14m) was very high and wind force was not so strong during study period, resuspension might not happen in the study area, especially during the particular period of study. So resuspension effect was not taking into account for the present study.

Input Boundary Conditions for Pathogen

The treatment plants and pumping stations around the study area discharge huge amount of pathogen into the Bay. Threre are 4 treatment plant stations (Shibaura, Sunamachi, Ariake and Morigasaki) in the study area which have a total of 28 pumping stations (Fig. 3.7). Each pumping station have different discharge rate. Onozawa *et. al*. (2005) was estimated discharge from each pumping station. According to that the daily total discharged water volume from 3 main treatment plant areas Shibaura, Sunamachi and Morigasaki is approximately 644000 ton, 415000 ton and 1198000 ton respectively. And 40% of Shibaura, 30% of Sunamachi and 65% of total water discharged from Morigasaki are polluted. So the volume of polluted water from Shibaura, Sunamachi and Morigasaki is 236000 ton, 131000 ton, 752000 ton respectively. Pumping stations of Ariake area are new and modern and don't discharge any significant amount of pollutants.

The total area of Shibaura treatment area is 6440ha, which consists of 6 different pumping stations. The area of each station is almost same. So we can roughly say each stations area is approximately 1000ha. We know that 40% of water discharged from this area. So if we multiply this volume with area (1000×0.40) we will get discharge of polluted water from each pumping station of Shibaura area. The area of Sunamachi and Morigashaki is 6153ha and 14675ha respectively. Thus we can calculate discharge from all the pumping stations.

Hellweger and Masopust in the year 2008 applied similar type of modeling to simulate E-coli in the Charles River, Boston, USA. In this study, they mentioned insufficient data were available to completely characterize *E. coli* concentration in the tributaries or develop such time-variable concentration models. Therefore, they used a constant *E-coli* concentration 3.5×10^7 CFU/100 ml.

In the present study the *E. coli* concentration in CSO was assigned 33×10^6 CFU/100 ml which is similar to that was used by Onozawa, *et. al*. (2005). This is also within the range for untreated wastewater (106-108 CFU/100 ml, Metcalf and Eddy, Inc., 2003).

Griffin *et. al*., 2003, found virus levels in wastewater 9.2×10^4 liter $^{-1}$. Based on this, in the present model the used AdV concentration is 1.0×10^4 per 100 ml.

However, this concentration will be diluted with rain water runoff (shown in the formula below) and eventually finds its way into the bay.

The formulas that were used to estimate pathogen discharge are as follows:

Water flow start time 5 min + Flowing time= Reach time
Flowing time= Length of pipe ÷ Flow velocity (1 m/s)
Length of pipe= $\sqrt{\text{Treating area}} \times 3/2$
Rain water runoff= Rainfall Amount× Treating Water Area (ha) ×
Water Flow co-efficient (0.8)

E.coli (CFU/100ml) = (33×10^6) × (Dry weather sewage) ÷ Rain Water Runoff)

Q= A×B/ 24*3600
A= Total treating polluted water volume (ton/day)
B= Area (each pumping station)
Q= Water discharge

Based on the above formula the result found is shown in the table 3.3

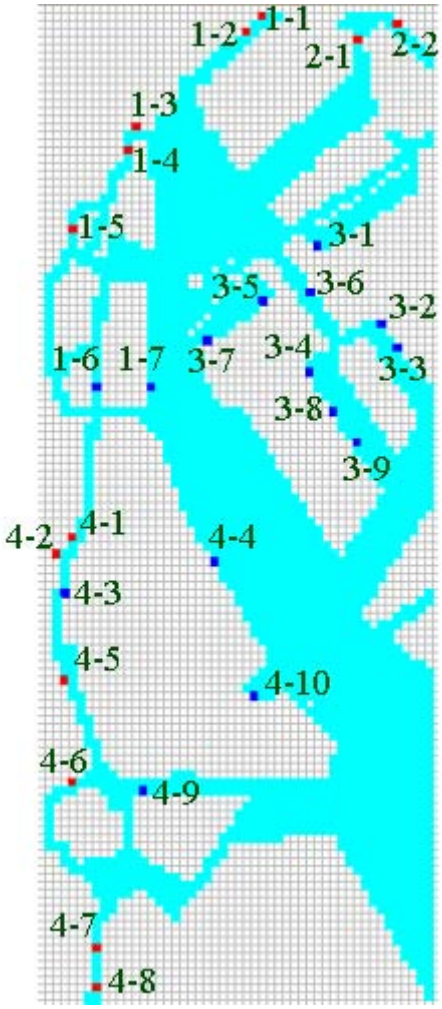

Sanitary pump station （19 site）

Storm water pump station （9 site）

(1) Shibaura area

(1-1) Sakurabashi
(1-2) Sakurabashi no2
(1-3) Akashimachi
(1-4) Shiodome
(1-5) Shiodome no2
(1-6) Shibaura
(1-7) Tennozu

(2) Sunamachi area

(2-1) Tsukudajima
(2-2) Echujima

(3) Ariake area

(3-1) Ariake north no2
(3-2) Ariake south no1
(3-3) Ariake south no2
(3-4) Daiba no1
(3-5) Daiba no2
(3-6) Aomi no1
(3-7) Aomi no2
(3-8) Chubo uchigawa
(3-9) Aomi Futo

(4) Morigasaki area

(4-1) Samezu
(4-2) Hamakawa
(4-3) Yashio
(4-4) Tokai
(4-5) Heiwajima
(4-6) Oomori Higashi
(4-7) Higashi Kojiya
(4-8) Haneda
(4-9) Keihinjima
(4-10) Jonanjima

Fig.3.7. List and position of pumping stations in the study area

Table 3.3. Volume of discharge pollutants from the pumping stations

		Area(km^2)	Reach time(min)	Assumed discharge (m^3/s)
Shibaura area				
	Sakurabashi	4.8	125	0.273
	Sakurabashi no2	4.8	125	0.273
	Akashimachi	6.4	165	0.364
	Shiodome	8	205	0.455
	Shiodome no2	8	205	0.455
	Shibaura	16	405	0.910
	Tennozu	8	205	0
	Shinagawa Futo	8	205	0
Sunamachi area				
	Tsukudajima	10	255	1.075
	Echujima	4	105	0.430
Ariake area				
	Ariake north	1	30	0
	Ariake south	1	30	0
	Ariake south	1	30	0
	Daiba no1	1	30	0
	Daiba no2	1	30	0
	Aomi no1	1	30	0
	Aomi no2	1	30	0
	Chubo	1	30	0
	Aomi Futo	1	30	0
Morigasaki area				
	Samezu	15	380	1.447
	Hamakawa	15	380	1.447
	Yashio	10	255	0
	Tokai	10	255	0
	Heiwajima	15	380	1.447
	Oomori Higashi	15	380	1.447
	Higashi Kojiya	15	380	1.447
	Haneda	15	380	1.447
	Keihinjima	10	255	0
	Jonanjima	10	255	0

3.4.3 Data source for model validation

In the present study the primary purpose of field observation was to validate the numerical model with the observed data. But the data was not sufficient due to difficulties in intensive monitoring. So that observed data was not used for validation. Instead of that a secondary observation data of *E. coli* and Adenovirus collected from the same study site (as discussed in chapter 3.2) during August to October 2004 (Fig. 3.8 and Fig. 3.9) were taken from Mr. Onozawa (previous student) to validate the model. Amount of rainfall at that particular period of modeling experiment was taken from Japan Meteorological Agency website (http://www.jma.go.jp) is shown in the table 3.4.

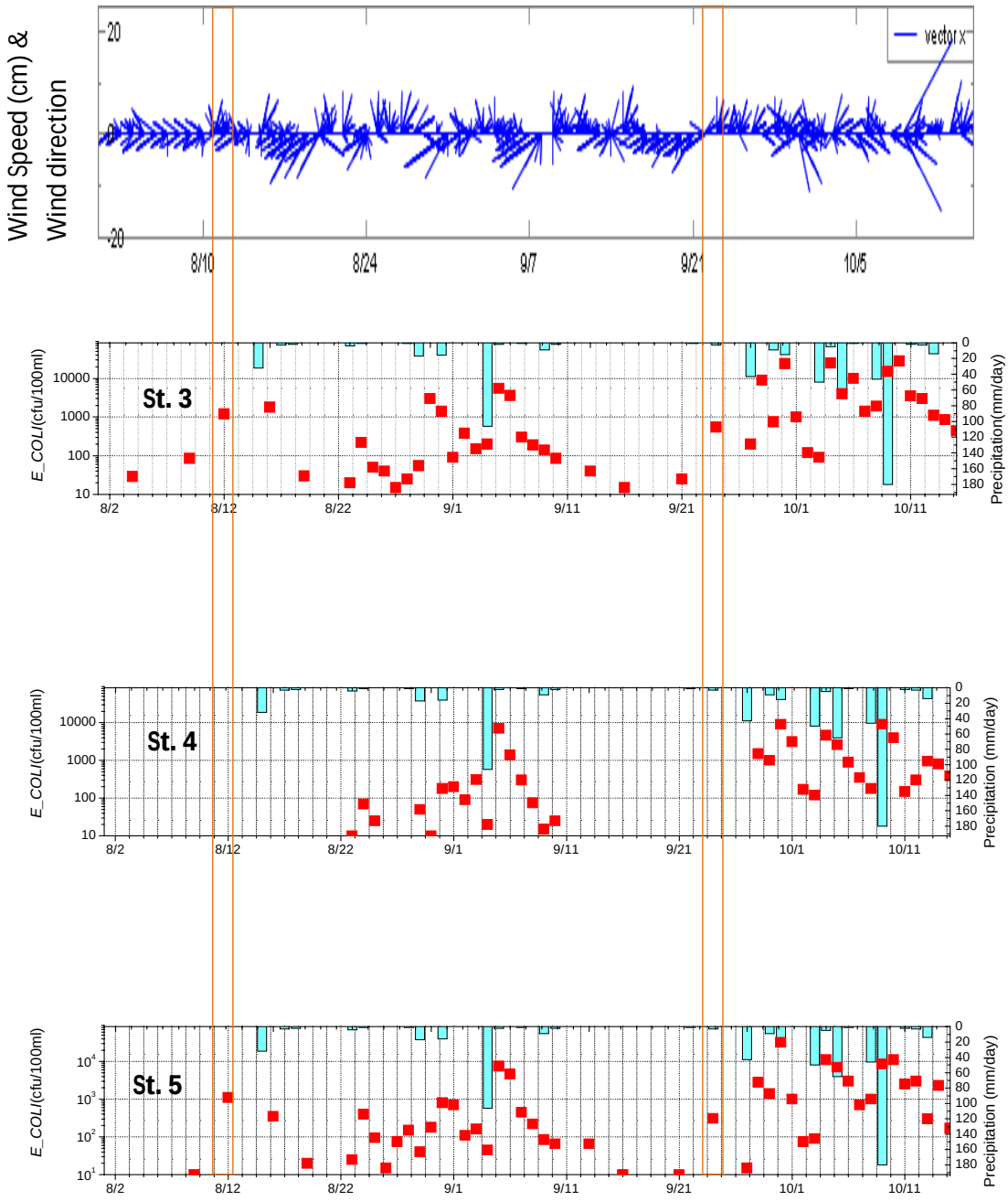

Fig. 3.8. Observed E. coli conc. with amount of precipitation at St. 3, 4 and 5 in 2004

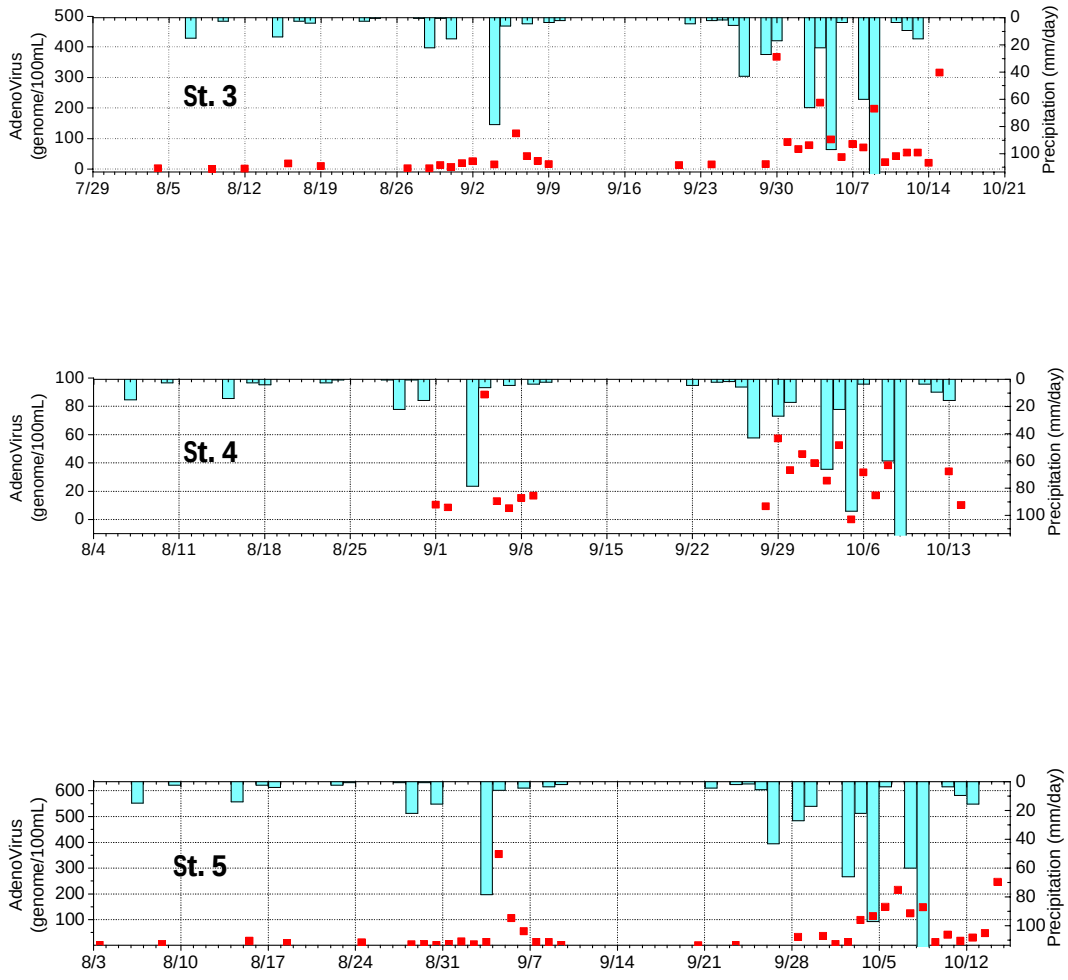

Fig. 3.9. Observed Adenovirus conc. with amount of precipitation at St. 3, 4 and 5 in 2004

Table. 3.4. Amount of rainfall during August to October 2004

Date	Rainfall (mm/day)	Date	Rainfall (mm/day)
2004.08.03	0.0	2004.09.09	0.0
2004.08.04	0.0	2004.09.10	0.0
2004.08.05	0.0	2004.09.11	0.0
2004.08.06	0.0	2004.09.12	0.0
2004.08.07	0.0	2004.09.13	0.0
2004.08.08	0.0	2004.09.14	0.0
2004.08.09	0.0	2004.09.15	0.0
2004.08.10	0.0	2004.09.16	0.0
2004.08.11	0.0	2004.09.17	0.0
2004.08.12	0.0	2004.09.18	0.0
2004.08.13	0.0	2004.09.19	0.0
2004.08.14	0.0	2004.09.20	0.0
2004.08.15	32.0	2004.09.21	0.0
2004.08.16	0.0	2004.09.22	1.0
2004.08.17	2.5	2004.09.23	0.0
2004.08.18	4.0	2004.09.24	3.0
2004.08.19	0.0	2004.09.25	0.0
2004.08.20	0.0	2004.09.26	0.0
2004.08.21	0.0	2004.09.27	43.0
2004.08.22	0.0	2004.09.28	0.0
2004.08.23	4.0	2004.09.29	9.0
2004.08.24	0.5	2004.09.30	15.0
2004.08.25	0.0	2004.10.01	0.0
2004.08.26	0.0	2004.10.02	0.0
2004.08.27	0.0	2004.10.03	50.0
2004.08.28	0.5	2004.10.04	5.0
2004.08.29	17.0	2004.10.05	0.0
2004.08.30	0.5	2004.10.06	65.0
2004.08.31	15.5	2004.10.07	*0.0*
2004.09.01	0.0	2004.10.08	46.0
2004.09.02	0.0	2004.10.09	180.0
2004.09.03	0.0	2004.10.10	0.0
2004.09.04	106.0	2004.10.11	2.0
2004.09.05	2.0	2004.10.12	3.0
2004.09.06	0.0	2004.10.13	14.0
2004.09.07	1.0	2004.10.14	0.0
2004.09.08	0.0	2004.10.15	0.0

CHAPTER 4: RESULTS

4.1 Field Observation 2007

4.1.1 Dissolved Oxygen

The dissolved oxygen concentrations in coastal waters shall not be less than 4 mgL^{-1}. Naturally occurring variations below the criterion specified may occur for short periods. These variations reflect such natural phenomena as the reduction in photosynthetic activity and oxygen production by plants during hours of darkness. However, no waste discharge or human activity shall lower the DO concentration below the specified minimum. These DO criteria are designed to protect aquatic life species associated with the aquatic environment (LDEQ, 2000).

According to Ministry of Environment, Japan's Environmental Quality Standards (EQS) for coastal water bathing and conservation of natural environment DO value is 7.5 mgL^{-1} or more.

The concentration below 4mgL^{-1} was found to be happened frequently, where the lowest value was recorded from the station 6 (2.26 mgL^{-1}). This indicates poor water quality of the Bay. The mean DO value was recoded as 4.17mgL^{-1}.

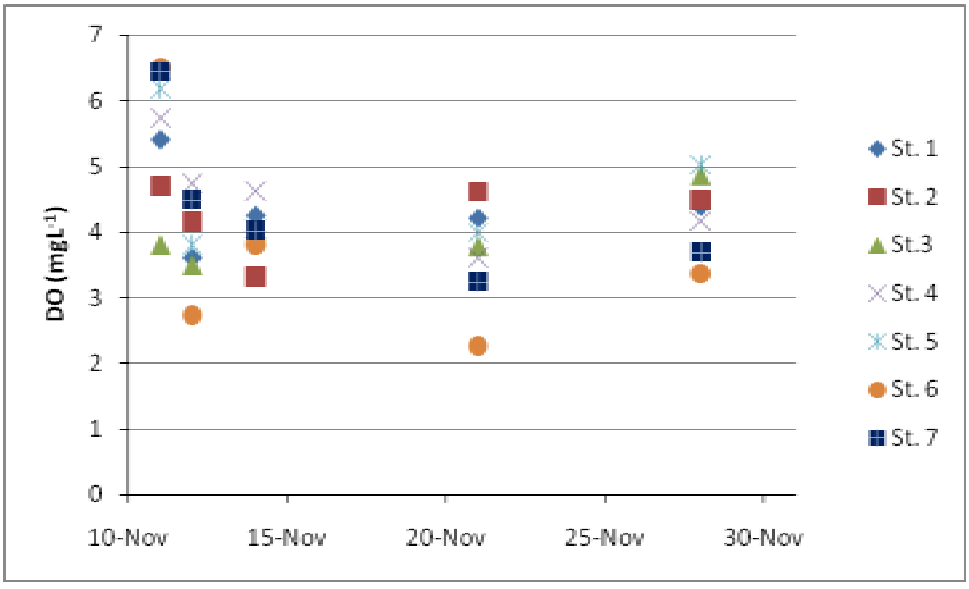

Fig. 4.1. Observed mean DO value from all the stations surface water, 2007

4.1.2 Temperature

Water temperature is very important as it exerts a major influence on the biological activity and growth of aquatic organisms. It has a great influence on water chemistry. The rate of chemical reactions generally increases at higher temperature, which in turn affects biological activity. The enzymes of most organisms work best at temperatures of 20-40^{0}C. An important example of the effects of temperature on water chemistry is its impact on oxygen. Warm water holds less oxygen than cool water, so it may be saturated with oxygen but still not contain enough for survival of aquatic life. Some compounds are also more toxic to aquatic life at higher temperatures. Un-ionized ammonia increments with temperature, becoming toxic to both plants and animals (McCorquodale, *et. al.,* 2005).

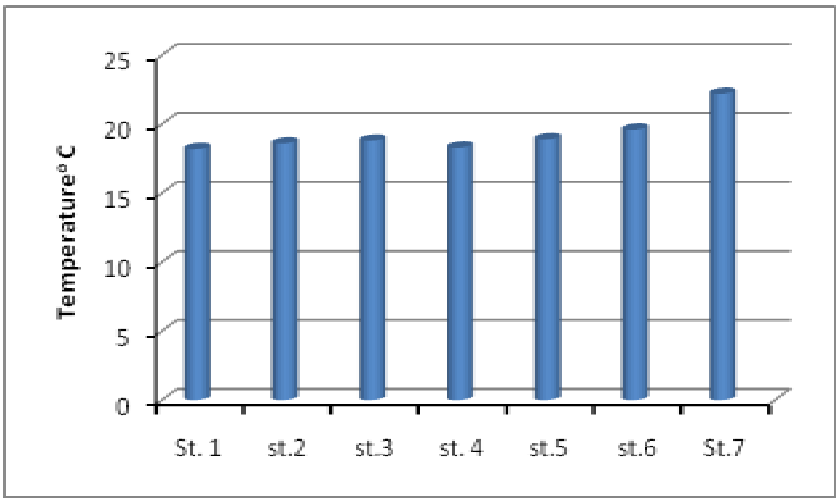

Fig. 4.2. Observed mean temperature from all the stations surface water

The mean temperature recorded in the sampling dates of November was 19.2^{o}C. The mean temperature at the St.1 was lower since the river water was cooler than Bay water. Temperature of St. 2 which is located near the Shibaura Water Reclamation Centre (WRC) was found higher. Otherwise, no obvious trend in water temperature was revealed.

4.1.3 Salinity

The mean Salinity values were lowest at the St. 1, St. 6 and St. 7 (20.3, 21 and 14.7 psu respectively). The salinity in the St. 1 was low due to its position near the mouth of Sumida River. The salinity of St. 6 was low as it is land locked location and St. 7 was the lowest may be due to discharge from Shibaura WRC.

4.1.4 Conductivity

The mean Conductivity and Specific Conductivities values were low at the stations 1, 6 and 7. This can be explained due to the proximity of these Stations to the mouth of the river where freshwater enters the lake and land locked position. The highest mean values for Conductivity were at station 2, 3, 4 and 5, which were located in the inner part of the Bay. This indicates that the Bay water that is least influenced by fresh water contained more dissolved salts, which are good conductors. Salinity and EC result was found very consistent and correlated (Fig. 4.3).

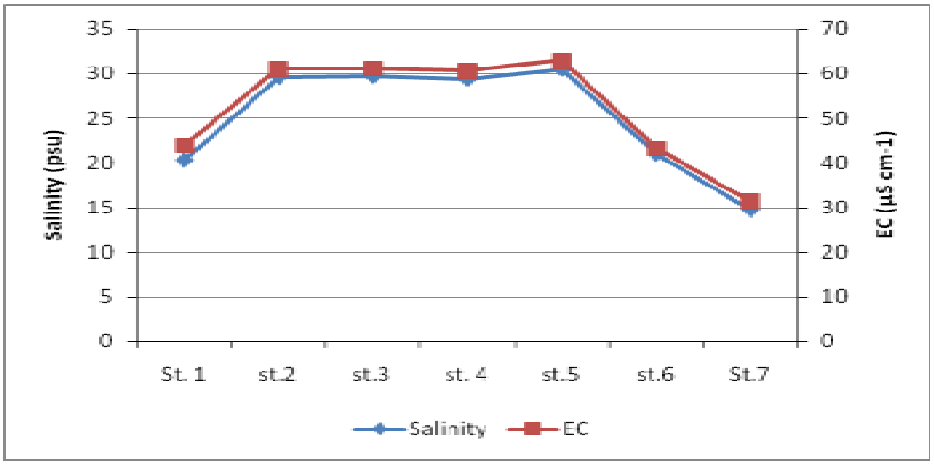

Fig. 4.3. Salinity and EC observed in different station during sampling

4.1.5 pH

The mean pH values for the station near the mouth of the river, was the lowest observed (pH 6.1). It indicates little bit acidic condition of river water. The pH values increased as one moved out and away from the mouth (Fig. 4.4). The mean surface water pH was found 6.75.

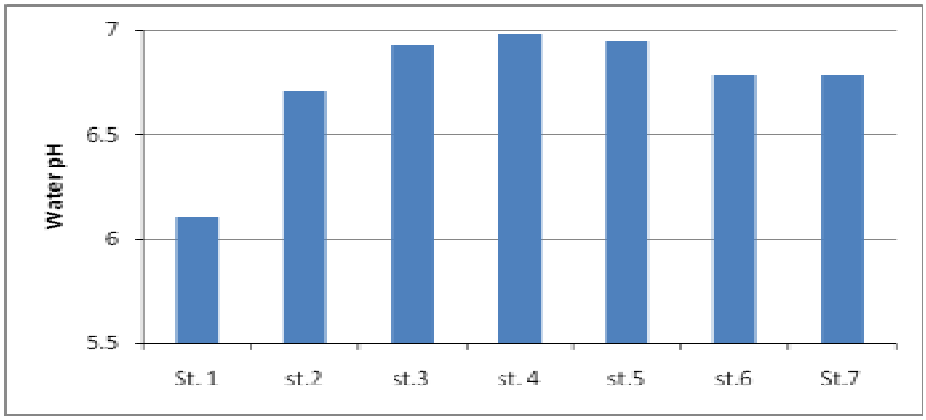

Fig. 4.4. Observed water pH at different stations

4.1.6 Turbidity and Suspended Solids (SS)

Figure 4.2, 4.3 and 4.5 shows Temperature, Salinity, Turbidity and Suspended Solids at the water surface obtained from the direct measurement. Water near the river outlet was of low-saline, high temperature and high SS and highly turbid. The reason for the high temperature was that river water was a little warmer than seawater in the season. Salinity gradually increased toward the open sea. There is a good positive correlation exists between observed Turbidity and SS (Fig. 4.6).

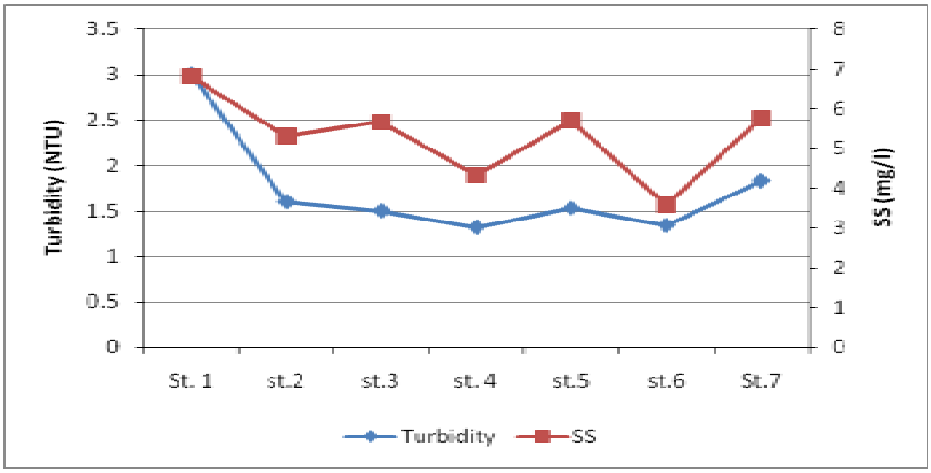

Fig. 4.5. Turbidity and SS observed in different stations during sampling

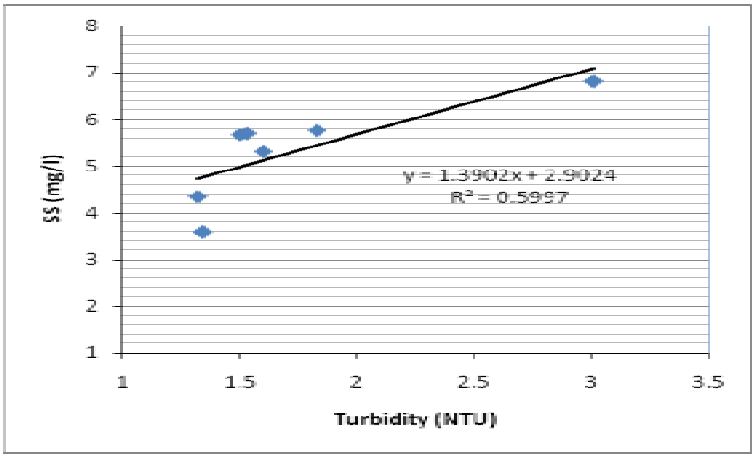

Fig. 4.6. Correlations between SS and Turbidity in the surface layer

Suspended particles (SS) in seawater play an important role in material transport. High turbidity layers in the vicinity of the bottom have been frequently observed in coastal areas and also on continental shelves and the large volume of suspended matter within these layers are believed to have a significant effect on material recycling processes. In coastal areas, resuspension and deposition of sediment due to tidal influences is predominant. Surface SS sink to the bottom going through river to the sea. Coagulations

and resuspension also occur near the bottom. Higher turbidity in the bottom layers of the stations (fig. 4.7) supports the above phenomenon.

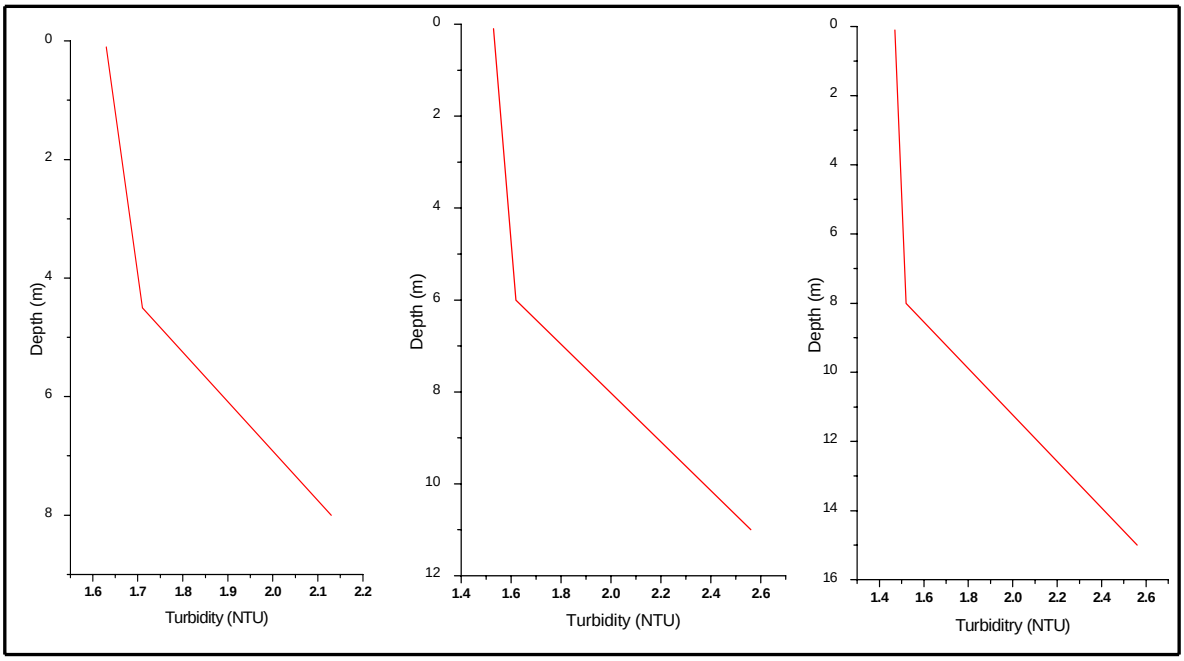

Fig. 4.7. Vertical distribution of Turbidity at St. 3(left), 4(middle) and 5(right)

Figure 4.8 shows the correlation between surface salinity and turbidity for all data obtained from the continuous measurement. This linear relation suggests that the process of turbidity decay along the bay axis was mainly caused by "dilution" of the dirty river water with the clean seawater, not by particle settling to a deep layer. It also suggests that the salinity distribution in the bay can be estimated by using turbidity as a tracer.

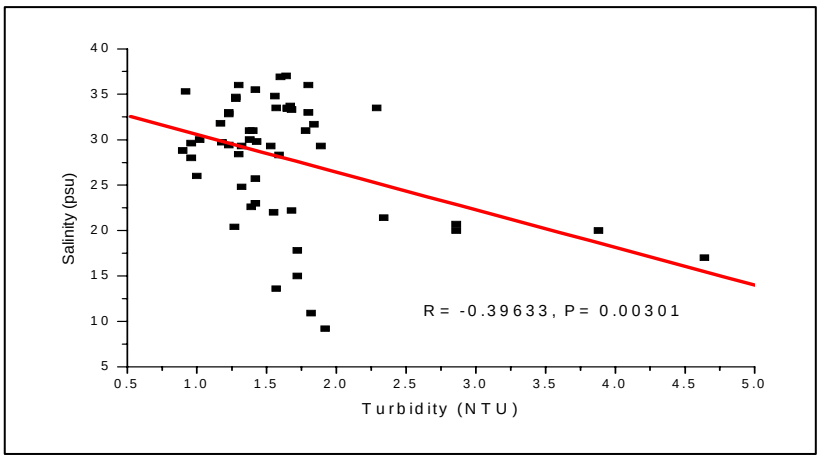

Fig. 4.8. Correlations between Salinity and Turbidity in the surface layer

4.1.7 Total Organic Carbon (TOC)

The temporal and spatial fluctuations of TOC were little with the average value of 2.6 mg/l for all samples. Figure 4.9 shows the spatial and temporal distribution of TOC.

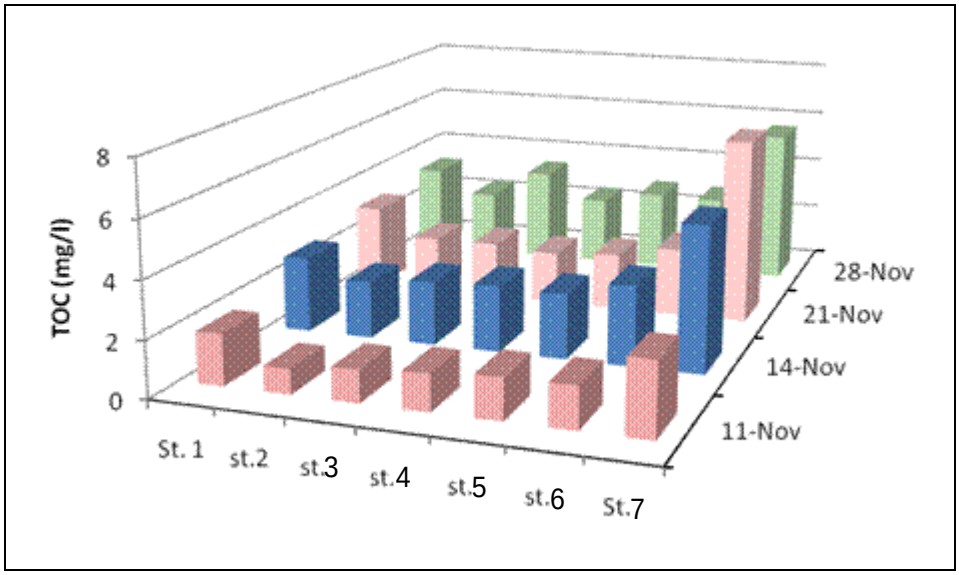

Fig. 4.9. Spatial and temporal variation of TOC

4.1.8 Nutrients

Nutrient levels during the background surveys were found higher at St.1 and St. 7 (Fig. 4.10). St.1 located near Sumida River and St. 7 near Shibaura Reclamation Centre. So even in normal day, without storm effect normal discharge from Sumida River and Shibaura Reclamation Centre may be the cause of higher nutrient level.

In all the cases surface nutrient have higher concentration (Fig. 4.11). Surface water less dilutes with sea water may be the cause. It was found to have inverse correlations among salinity and nutrients (Fig. 4.12).

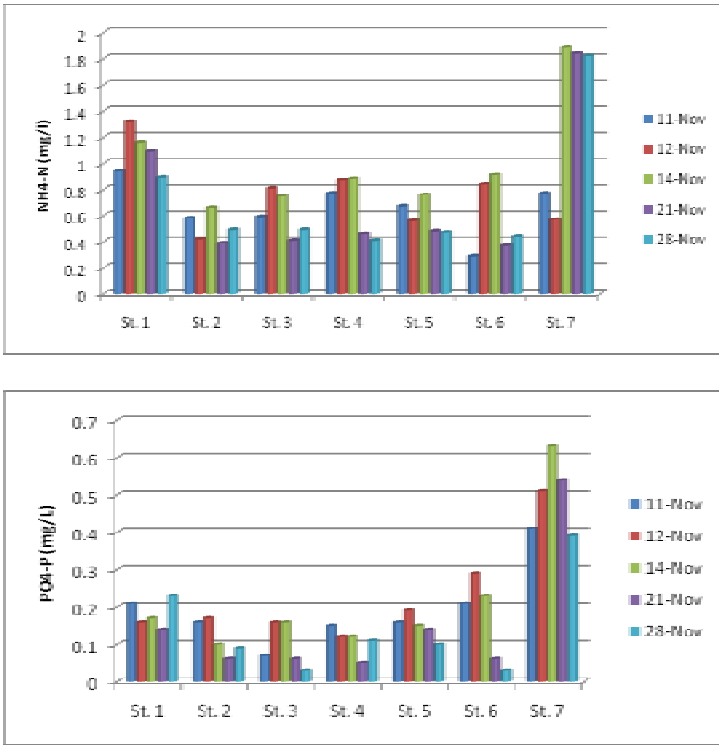

Fig. 4.10. Spatial and temporal variation of NH_4–N and PO_4–P during low tide

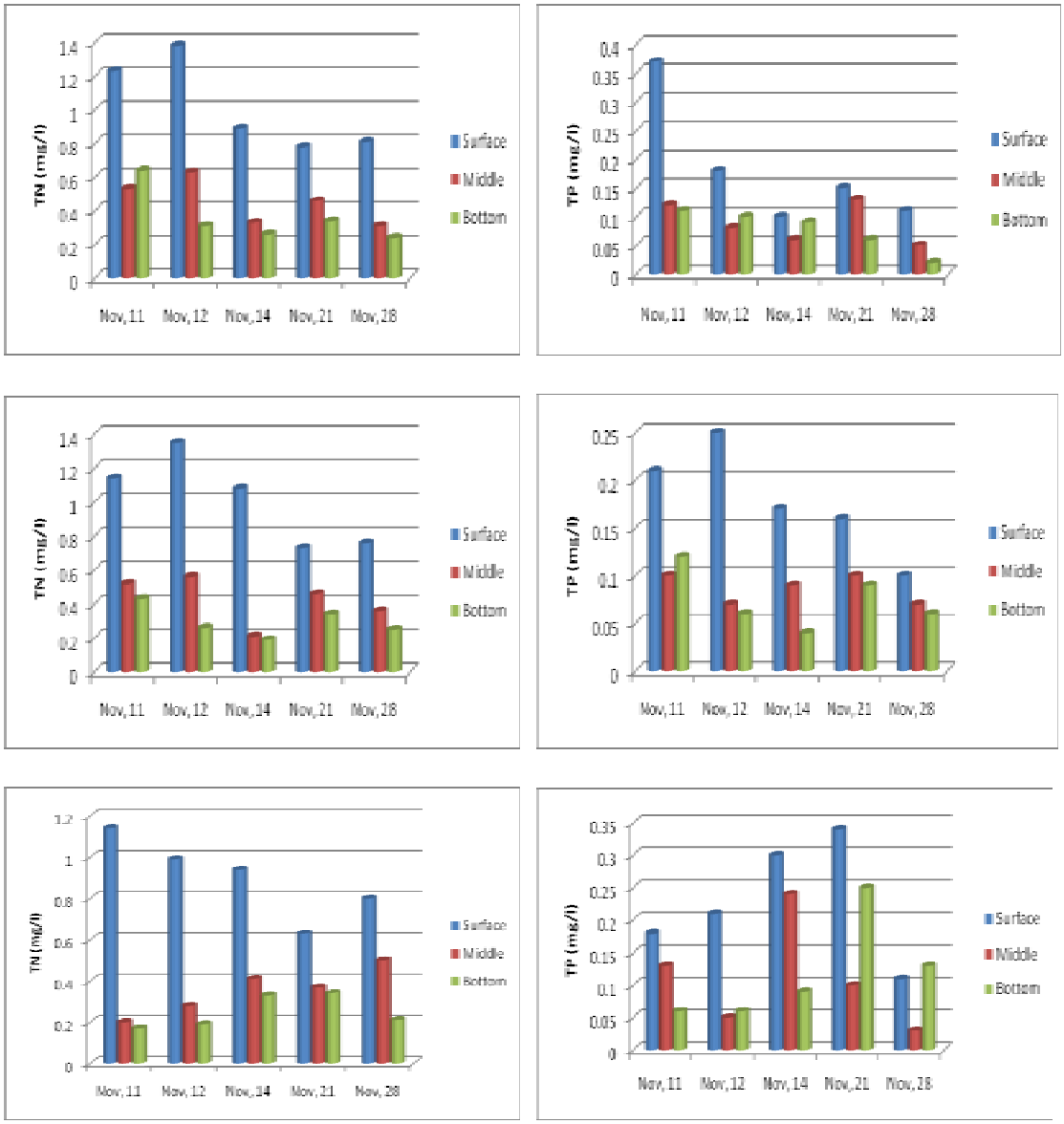

Fig. 4.11 Vertical distribution of water nutrient at St. 2 (upper), St. 3 (middle) and St. 5 (Lower) during low tide, 2007

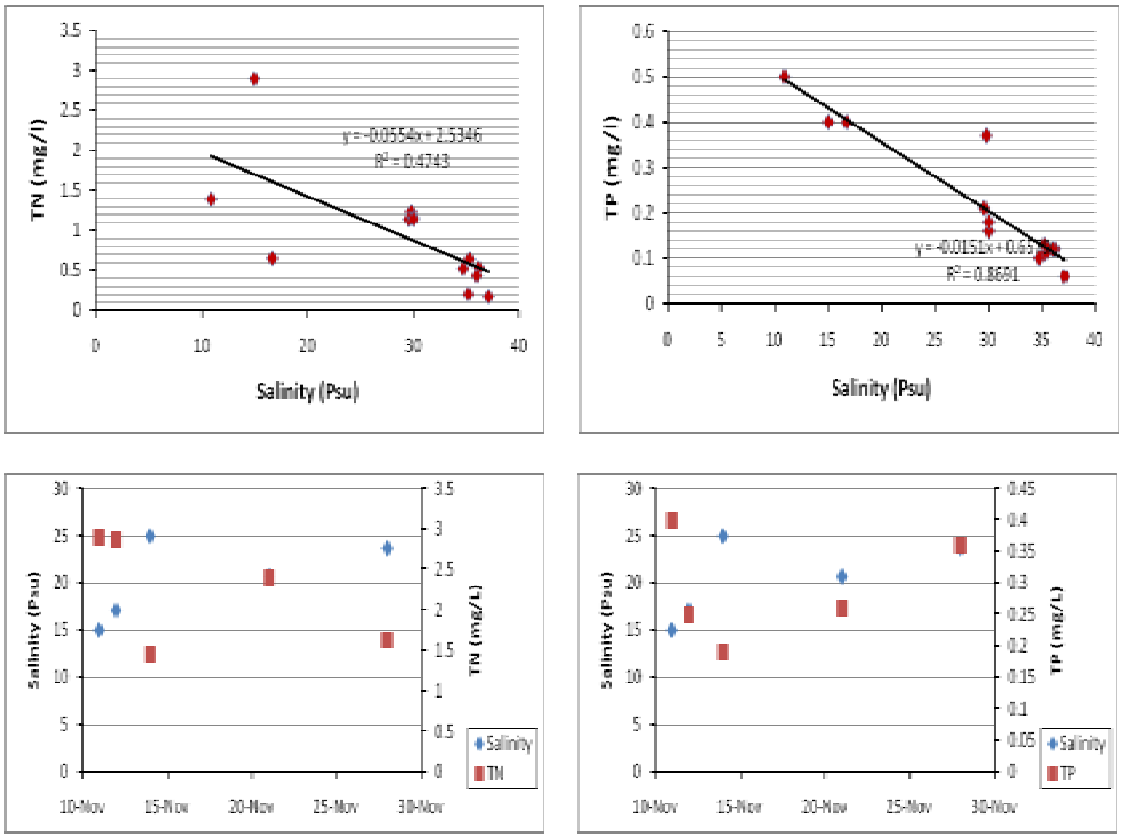

Fig. 4.12. Co-relation between Salinity and nutrient. Upper graphs show Nov 11, at all stations and graphs below is St.1 at all the sampling days during low tide, 2007.

4.1.9 Pathogen

According to Ministry of Environment, Japan the standard of bathing for Fecal Coliform is 1000 (CFU/100 mL) and according to US EPA that is 235 (CFU/100mL). Though Fecal Coliform includes not only *E. coli*, in this area majority comes from *E. coli.*

Figure 4.13 shows that just after 26.5 mm rainfall of Nov 10, concentration of *E. coli* and AdV increased tremendously and surpluses the standards. After 2 days the plume was found decreased again. Concentration at some stations increased again in normal days (Nov. 21 and 28) may be due to re-suspension from sediment or dry weather discharge from the STPs or input from any other sources. Figure 4.14 shows that concentration decrease with distance from the source of discharge.

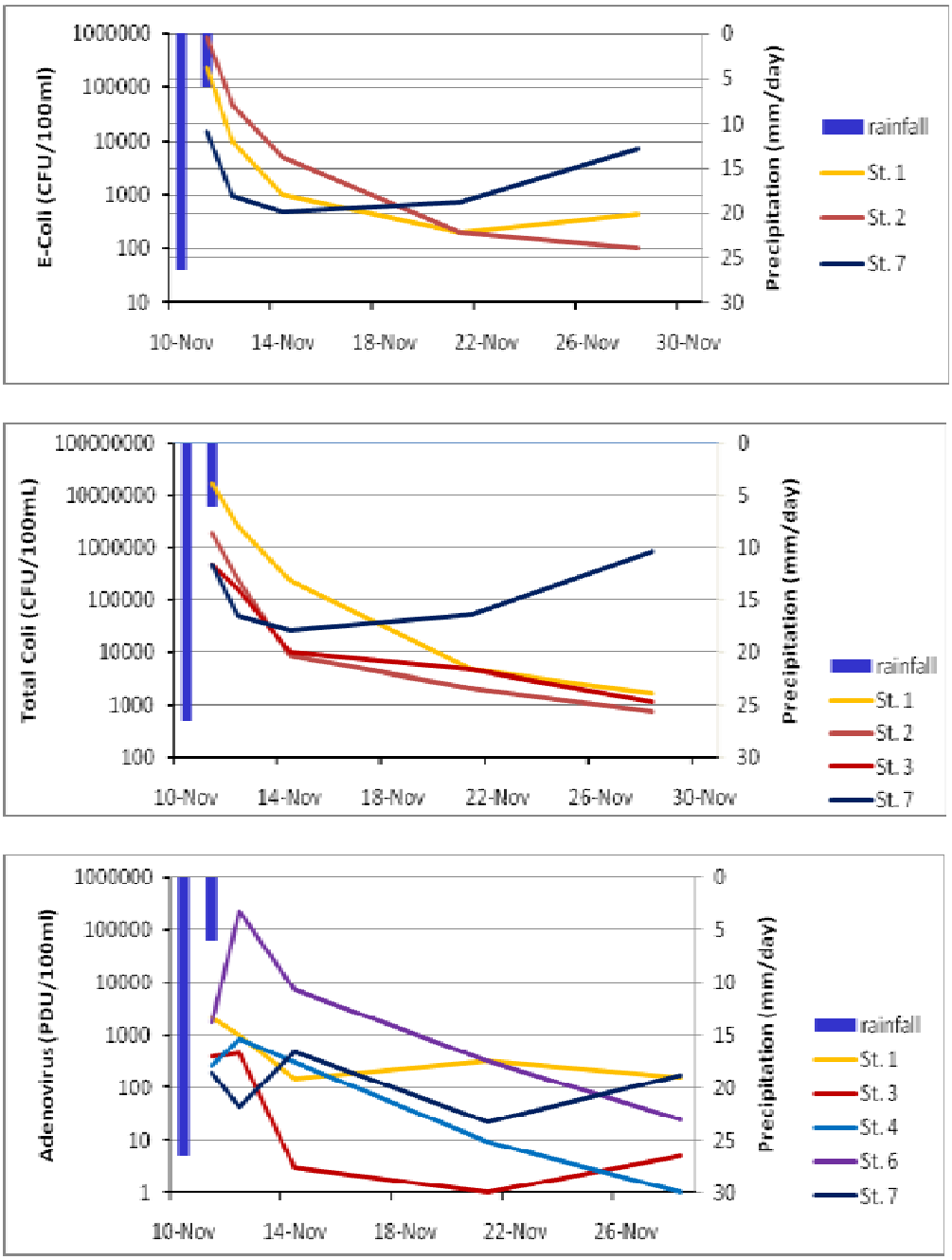

Fig. *4.13. Spatial and temporal variation of pathogen observed in 2007*

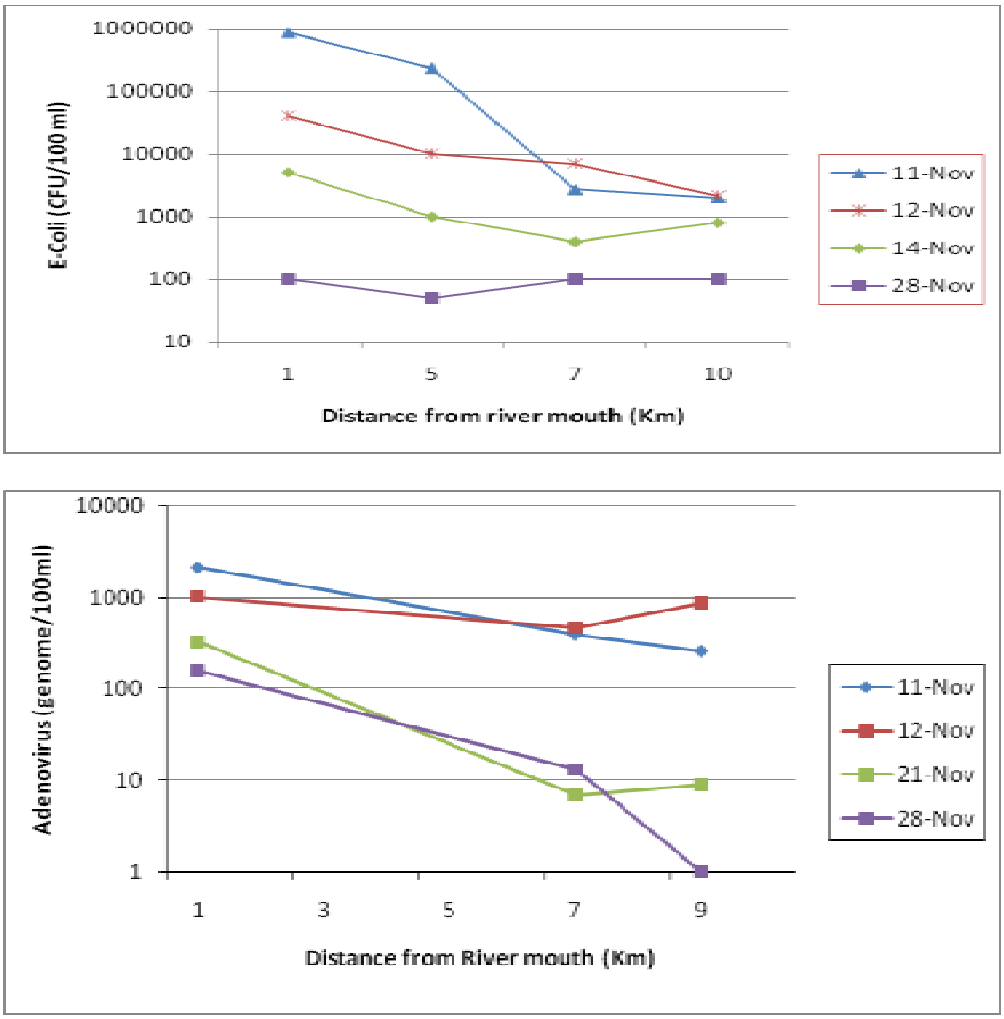

Fig. 4.14. Distribution of pathogen with distance from Sumida river mouth observed in 2007

4.2 Model calibration
4.2.1 Bay-wide model calibration

The hydrodynamics in the Bay-wide model (domain 1, large grid) were first simulated and the results of temperature, salinity and water surface level elevation were used as an open boundary to simulate domain 2 (fine grid). The model was simulated and validated by comparison with the observed data for a period of two and half months from August 1st to October 15th, 2004. The output result was presented in an hourly basis. The simulation and observation results of temperature and salinity patterns in the Bay-wide scale grid are shown in the Fig. 4.15 and Fig. 4.16 respectively. The simulation results show stratification, mixing, and an upwelling phenomenon.

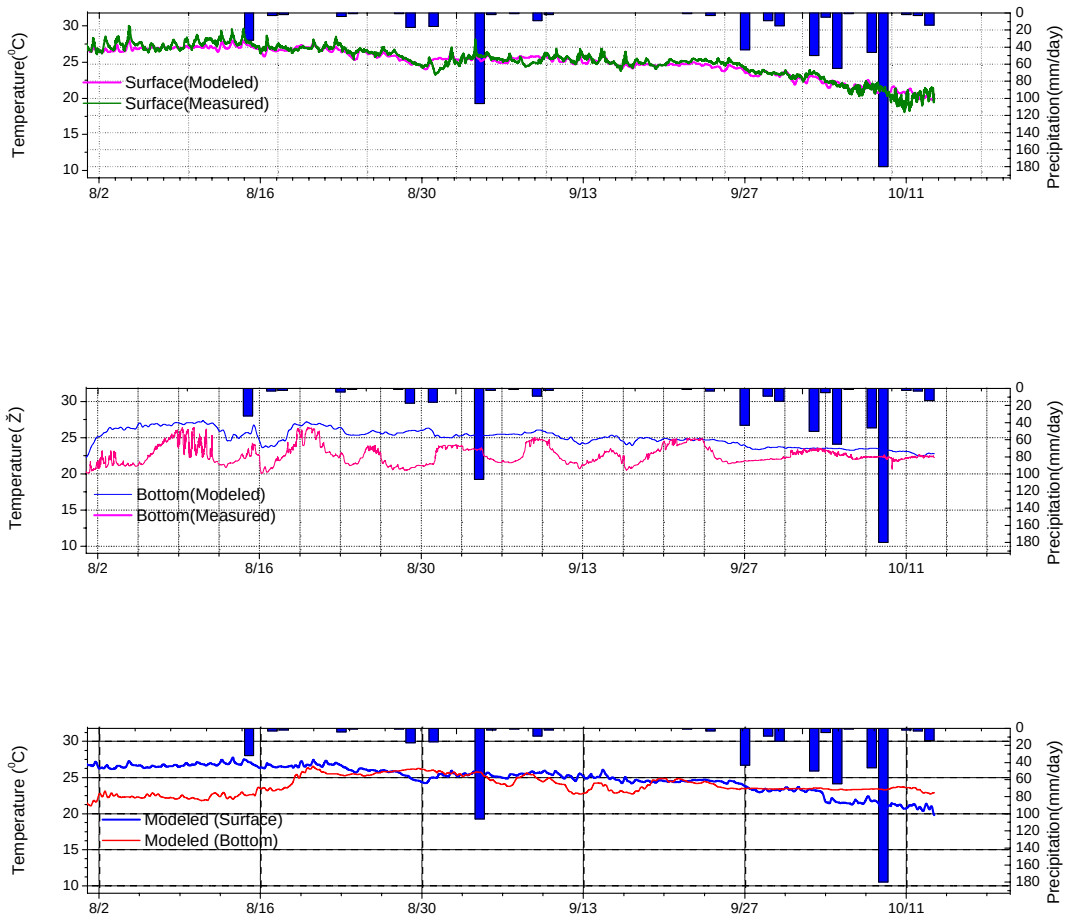

Fig. 4.15 Comparison between modeled and measured temperature at surface and bottom (depth was 12 m) near downstream of Odaiba, Tokyo Bay (2004)

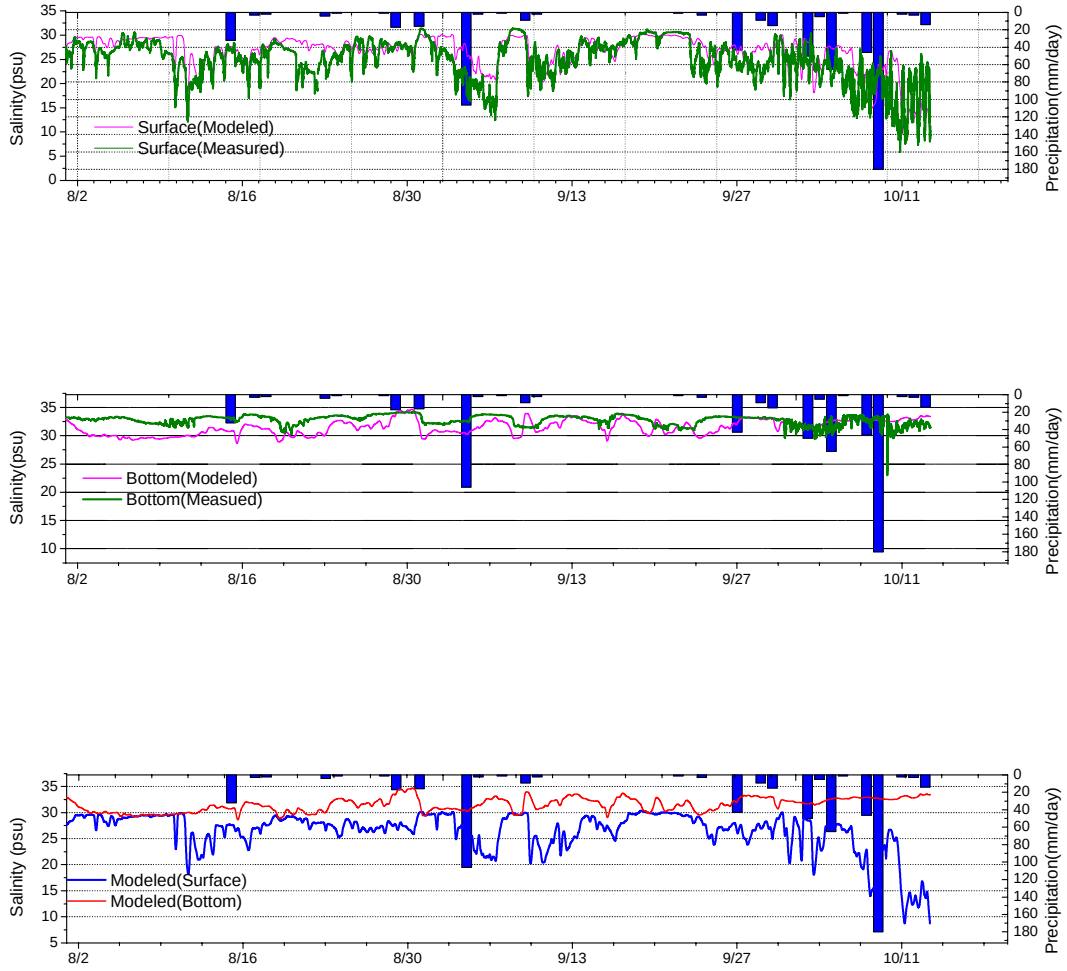

Fig. 4.16. Comparison between modeled and measured Salinity at surface and bottom (depth was 12 m) near downstream of Odaiba, Tokyo Bay (2004)

4.2.2 Fine grid model calibration

a) Temperature and salinity calibration

A comparison between observation and a calculation results are shown in figure 4.17 for temperature and figure 4.18 for salinity in a fine grid scale (domain 2 in Fig. 3.5). Variations between the simulated and observed values were generally less than 2.5°C and 2 psu through the water column. The timing and periods of upwelling events were captured accurately. After rain fall, river discharge was increased remarkably. Model results adequately represent precipitation variation events and their effects.

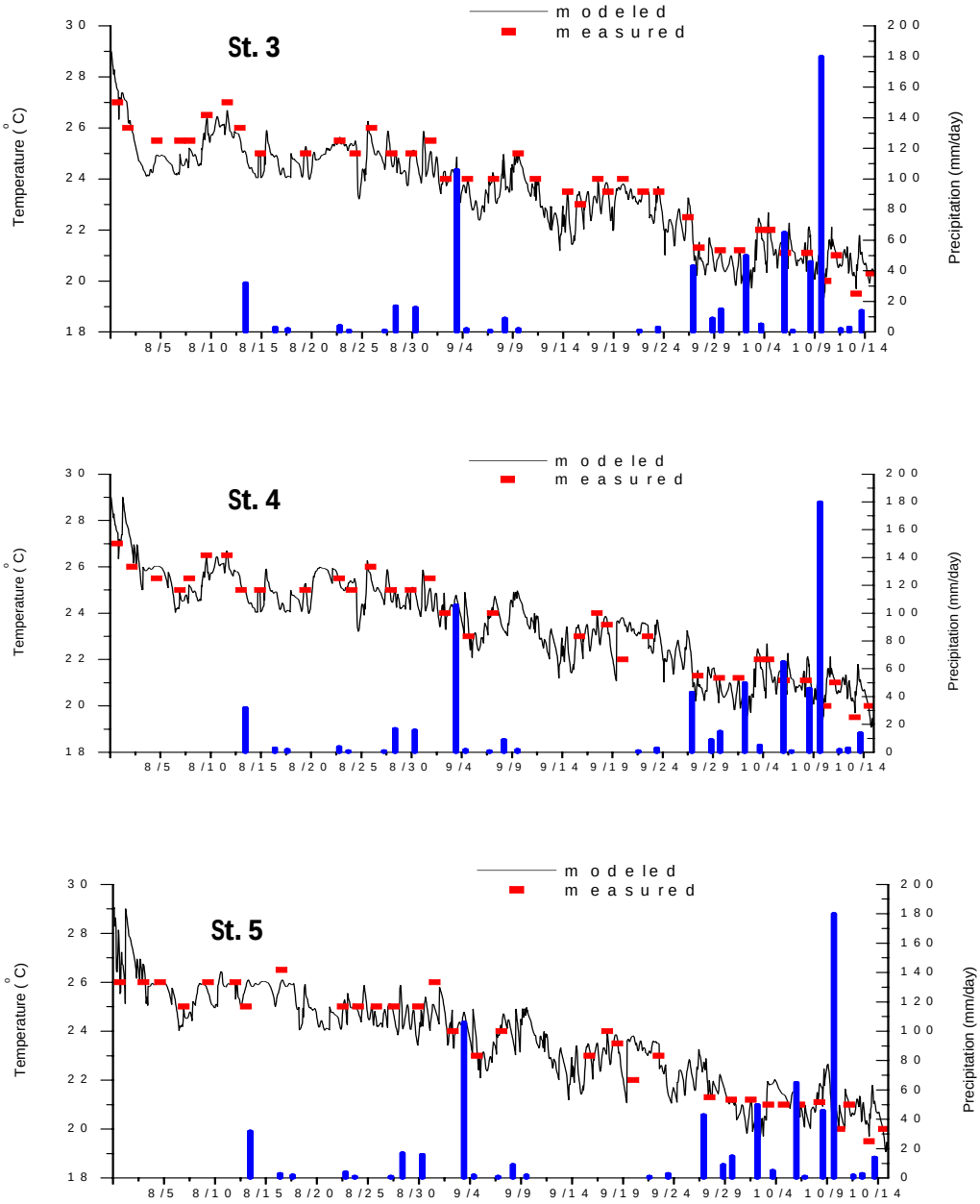

Fig. 4.17. Comparison between modeled and measured Temperature at surface water (2004)

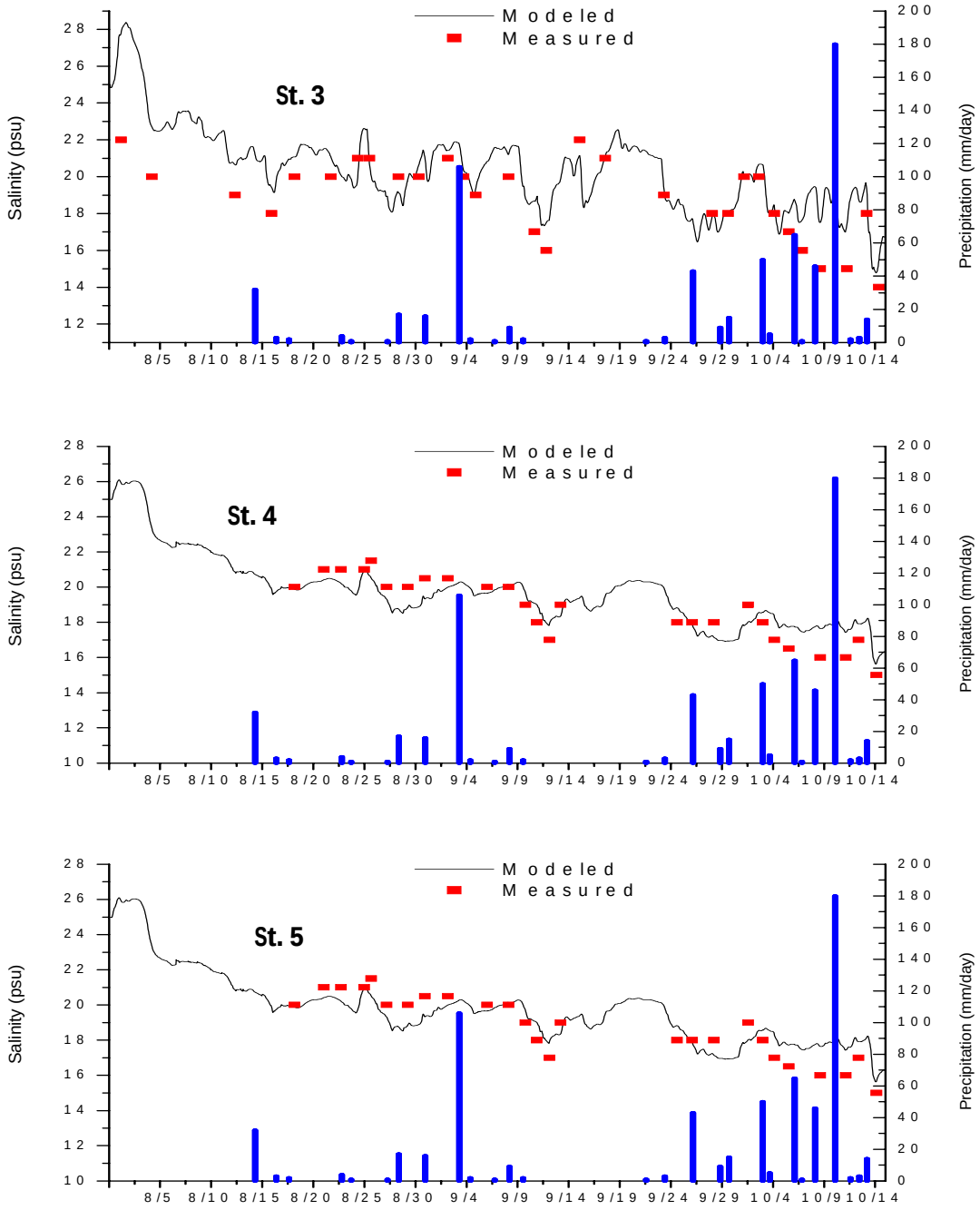

Fig. 4.18. Comparison between modeled and measured Salinity at surface water of Odaiba (2004)

b) Calibration of E. coli

Figure 4.19 shows a comparison between modeled and measured *E. coli*. The *E. coli* concentrations appeared to be significantly different among the stations. However, St. 3 and St. 5 show relatively higher concentration than St. 4. It may be due to the enclosed bathymetry of St.4. As St. 4 located comparatively more land locked position (near Daiba Kaihin Park), in this place wind force is not so strong like station 3 and 5. Again concentration also depends mainly on the river discharge, pumping station discharge and discharge from sewage treatment plant (STP). St. 3 and 5 contains higher discharge from river and STPs, due to their closest proximity and open position.

The temporal variability of concentration occurred due to mainly storm with CSO discharge. The main rainfall induced CSO discharge were occurred on August 15 (32mm), August 29 (16mm), August 31(16 mm), September 4 (106mm), September 30 (15mm), October 5 (65mm) and the biggest one on October 9 (180mm) leaded to higher concentrations. The result also reveals that the increasing rates of *E. coli* do not agree with levels of precipitation. Even in small precipitations, *E. coli* significantly increased.

c) Calibration of Adenovirus

To verify if the model was generating similar AdV concentrations as those observed in the field, the AdV concentrations from the field and the model were presented graphically (Fig. 4.20). This was a check on the mass of the pollutant loading. Moreover, if there was any difference in the orientation of the predicted plume and the plume observed in the field, this check would verify whether the model can actually predict the concentrations observed in the field.

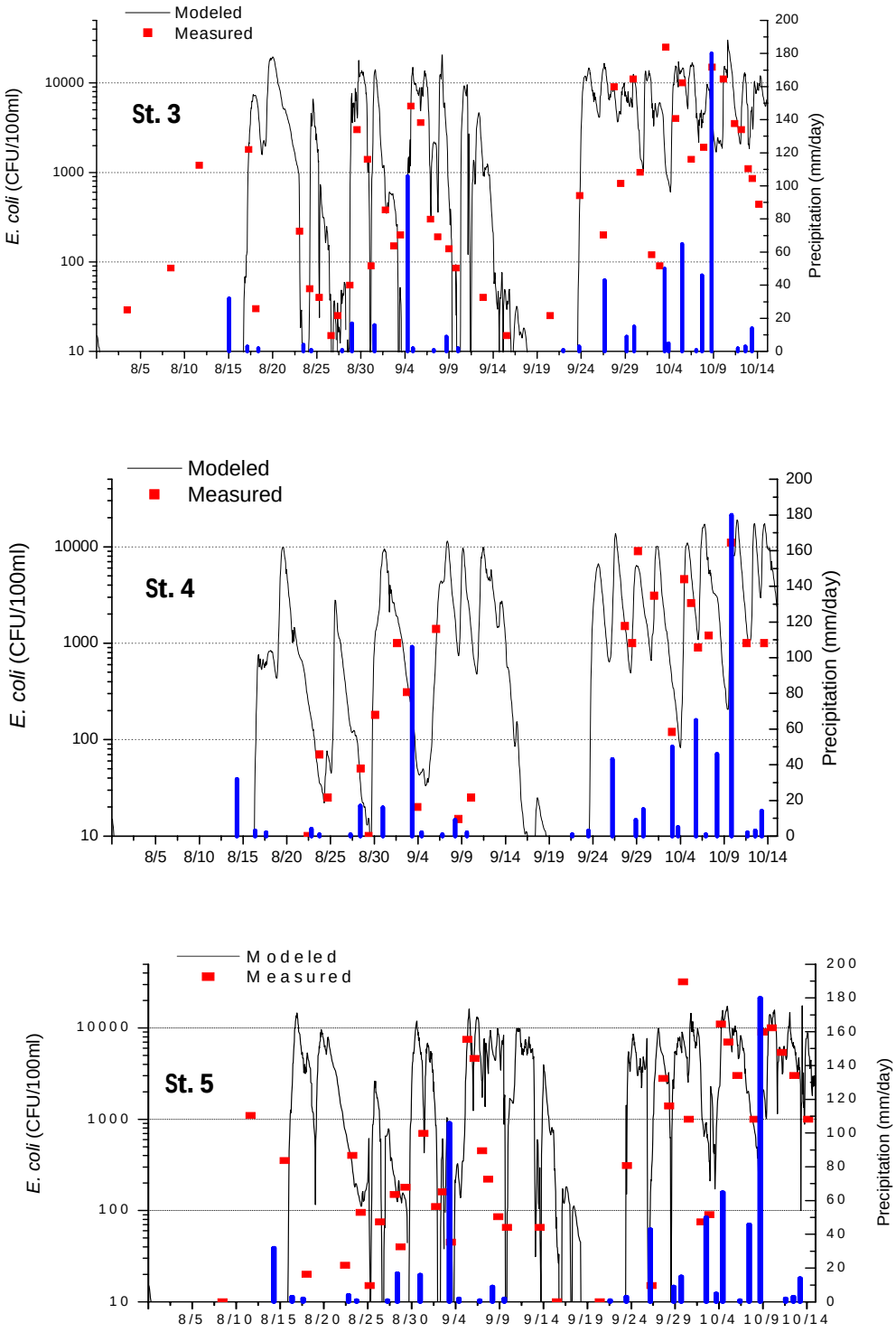

Fig. 4.19 Comparison between modeled and measured E. coli at surface water of Odaiba (2004)

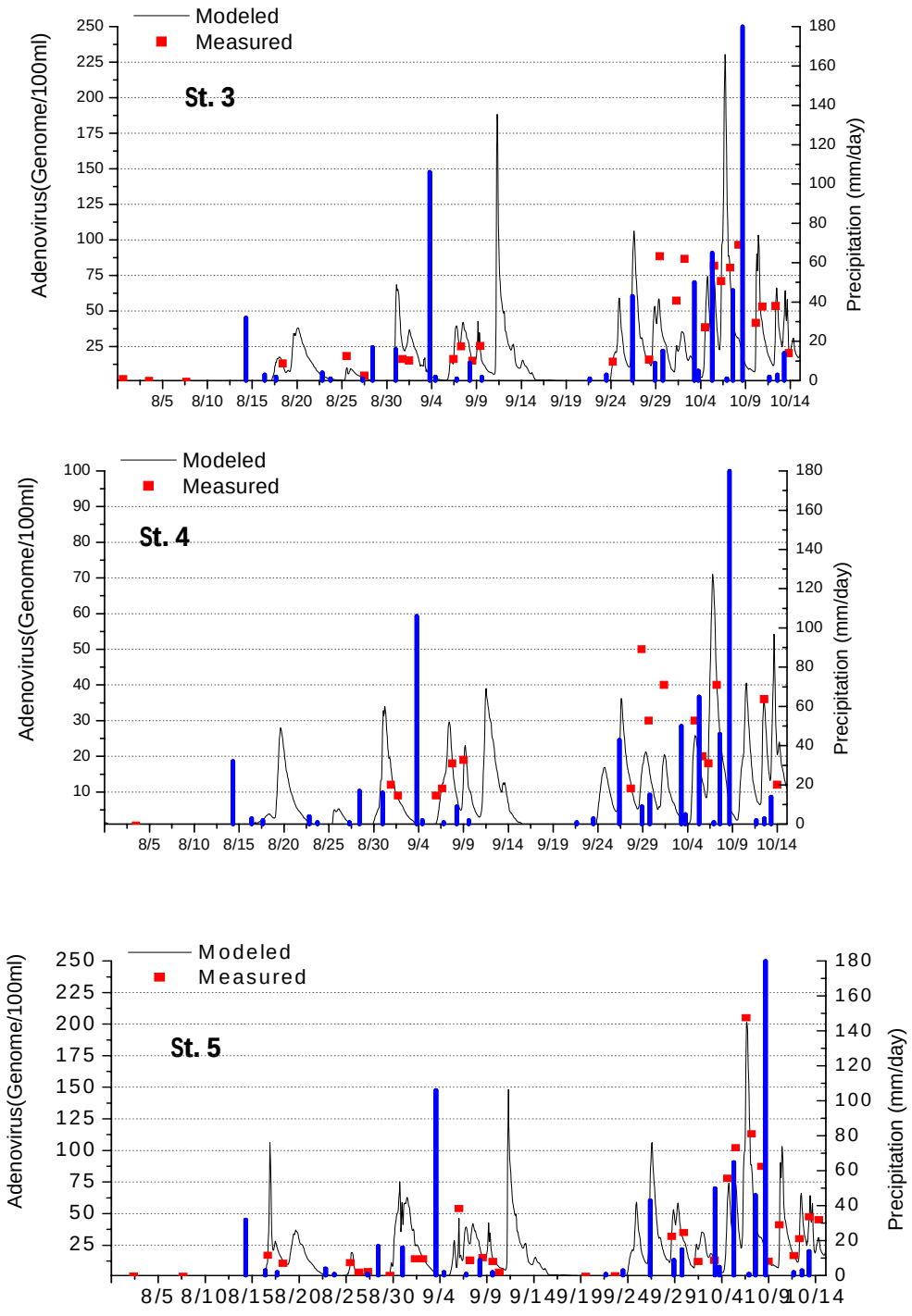

Fig. 4.20. Comparison between modeled and measured AdV at surface water of Odaiba (2004)

4.3 Numerical experiment

Variations in levels of *E. coli* are directly correlated with the discharge from pumping stations, tidal currents, river discharges, wind velocity and density distributions. Death rate also affects pathogen concentration significantly. As a result, the distributions of CSO differ according to timing, even when the level of discharge is the same (Onozawa *et. al.,* 2005).

Numerical experiments were performed for without death rate and no wind action case. The model captures the increase in *E. coli* concentration when the death rate was omitted (Fig 4.21) and concentration decrease when there was no wind velocity (Fig. 4.22). The same type of result was also found for AdV (Fig. 4.23).

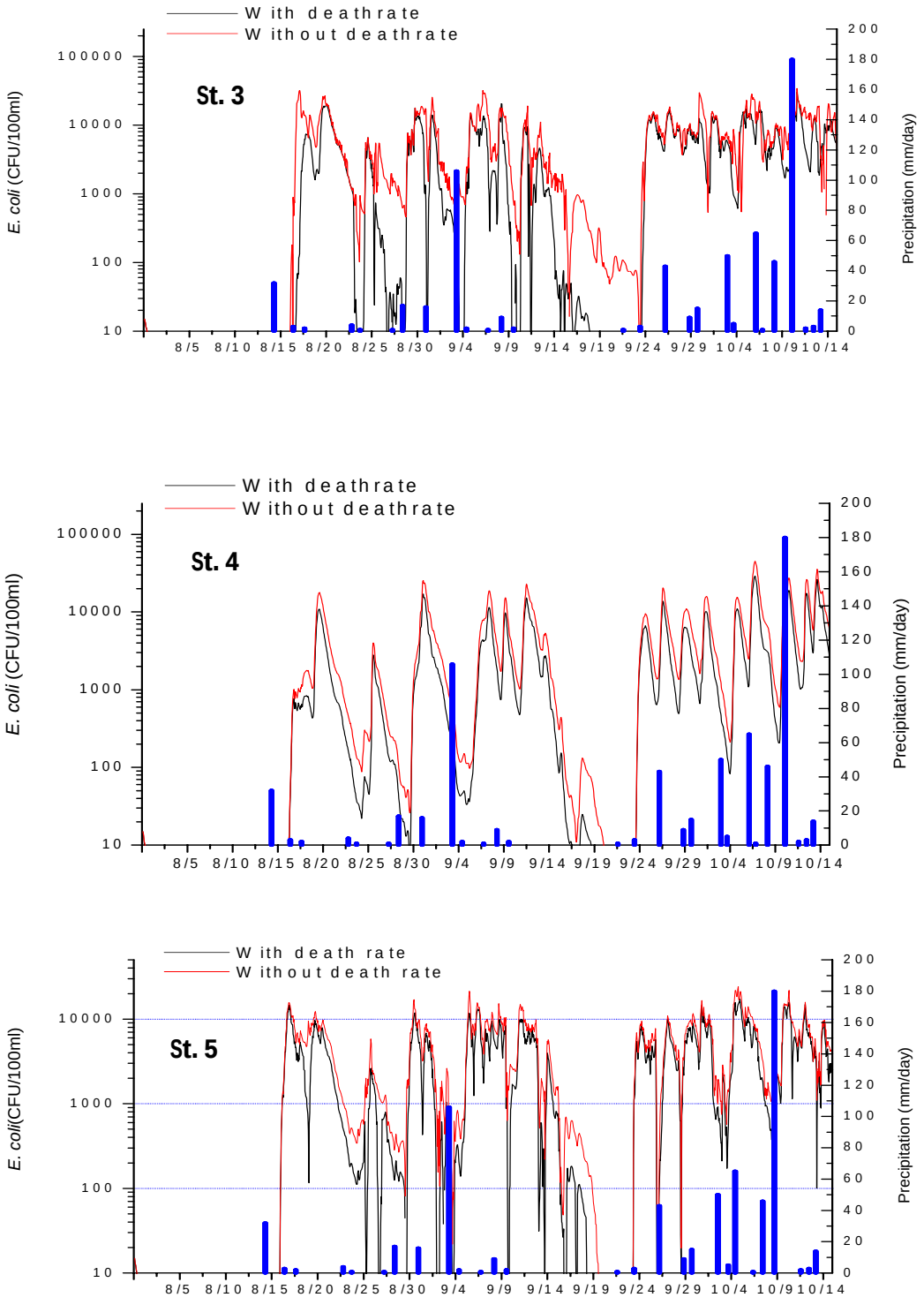

Fig. 4.21 Comparison between with and without death rate result of modeled E. coli conc.

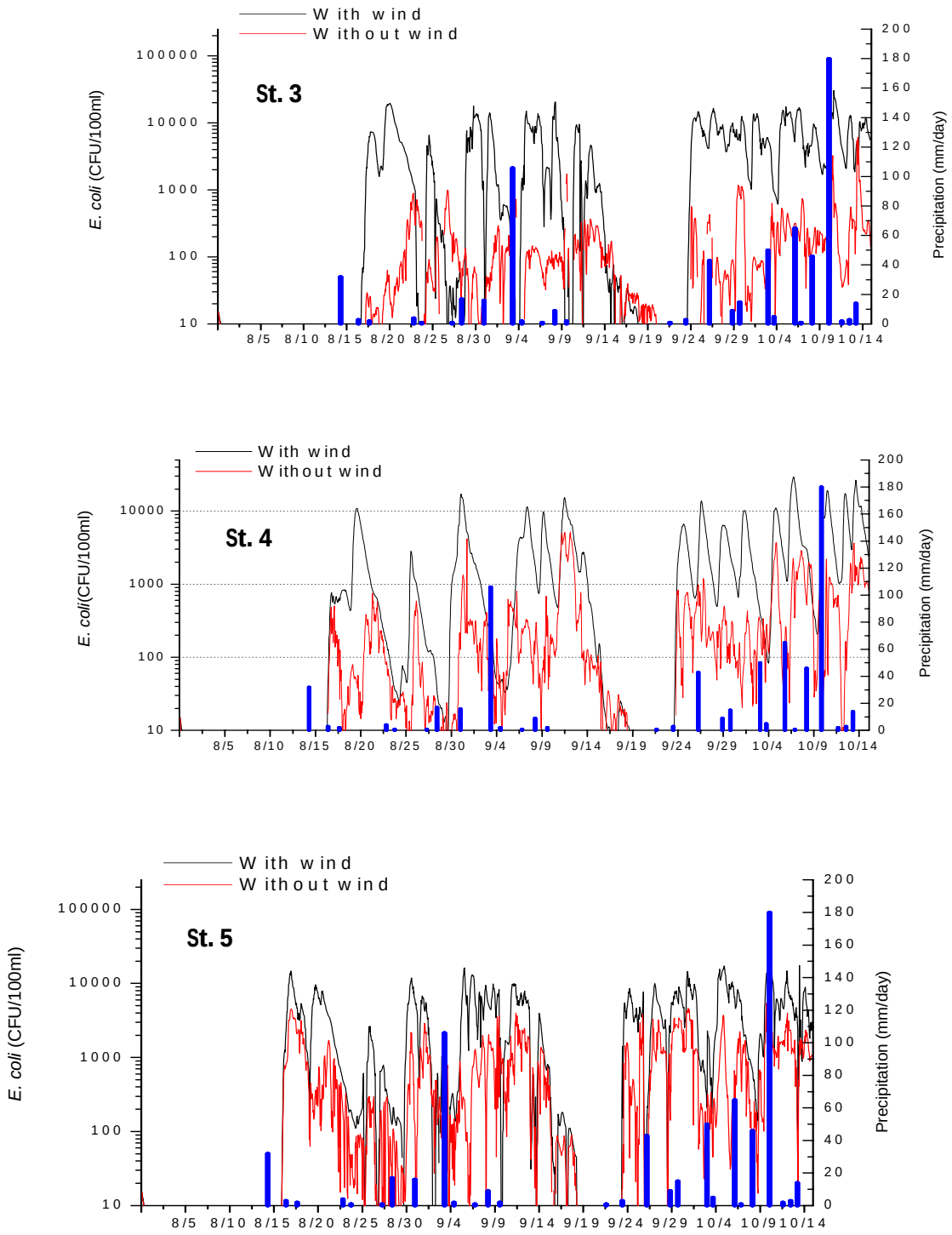

Fig. 4.22. Comparison between with and without wind action result of modeled E. coli conc.

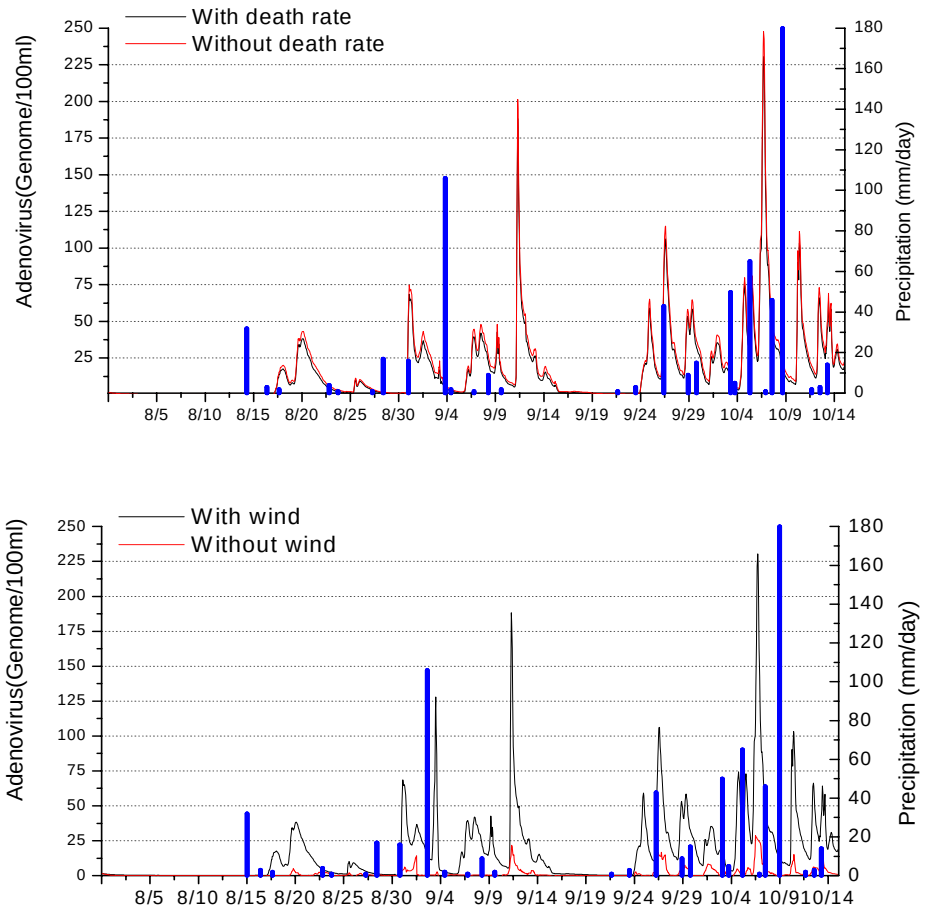

Fig. 4.23. Comparison between with and without death rate (up) and with and without wind action (down) result of modeled AdV concentration at St. 3 (2004)

4.4 Nowcast simulation of pathogen

Figure 4.24 shows temporal variations tidal levels and Pathogen concentrations. Pathogen come in Odaiba area from three different treatment plant areas. Shibaura and Sunamachi area are located at the upper bay location from the Odaiba area. Morigasaki has the largest area, but is located in the lower bay location from the Odaiba area (See Fig. 3.1). In this spring tide period, Small precipitation (16mm/hr) was measured at August 29th. The levels of *E. coli* and AdV increased rapidly after the rainfall event, due mainly to discharges from all the 3 STPs. As it was spring tide period tidal ranges was reached 200 cm. So effluent from Morigasaki also reached the Odaiba area.

In contrast, figure 4.25 shows a large precipitation (180mm/hr) case under the neap tide period. In this period, only the upper bay's CSO's arrived at the Odaiba area. No

contributions from the Morigasaki area took place. So it is found that pathogen concentrations reached maximum levels after small precipitation events, but did not increase that much under large precipitation event.

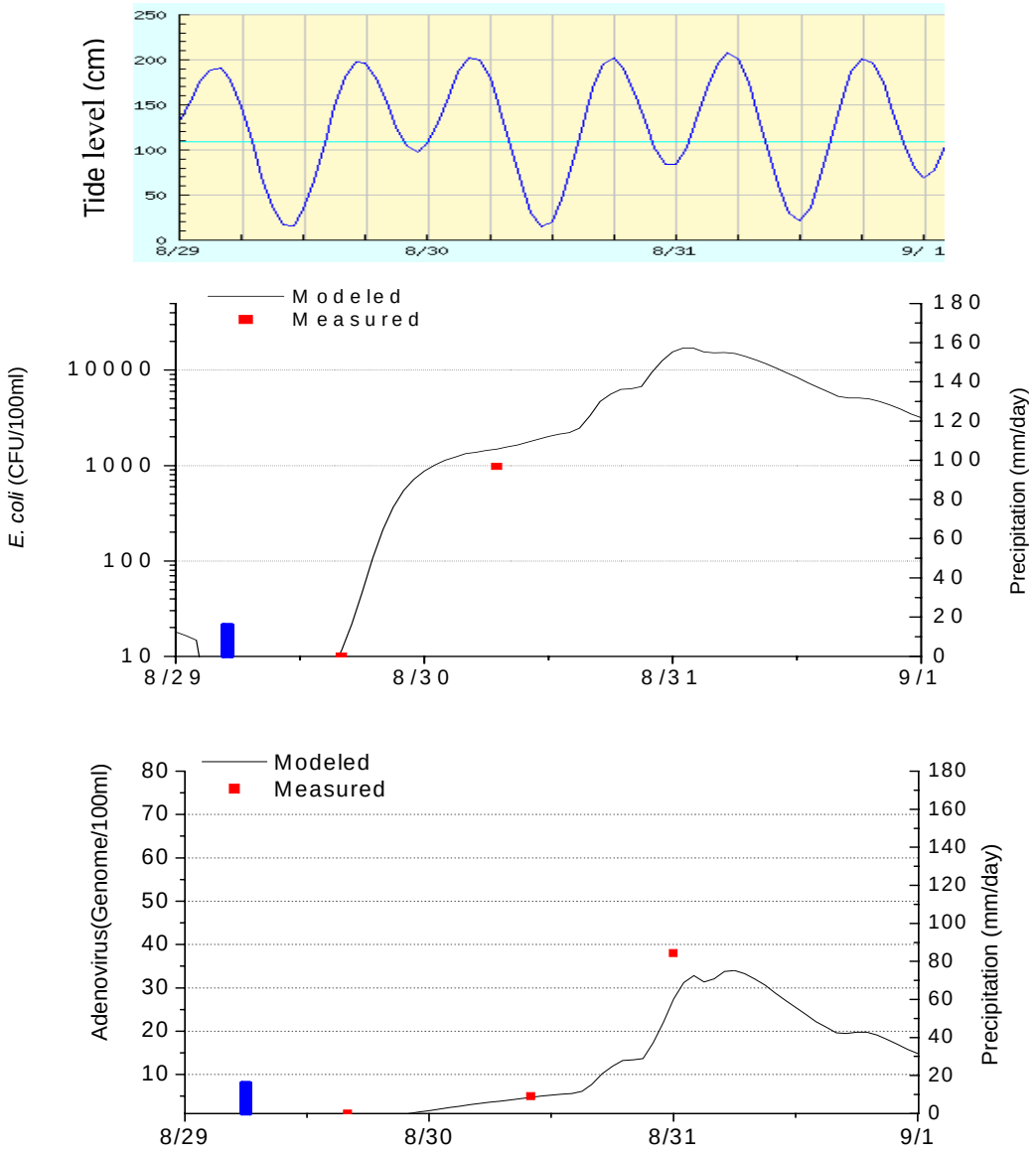

Fig. 4.24. Effect of rainfall and tides for Pathogen variations under the small storm event at St.4

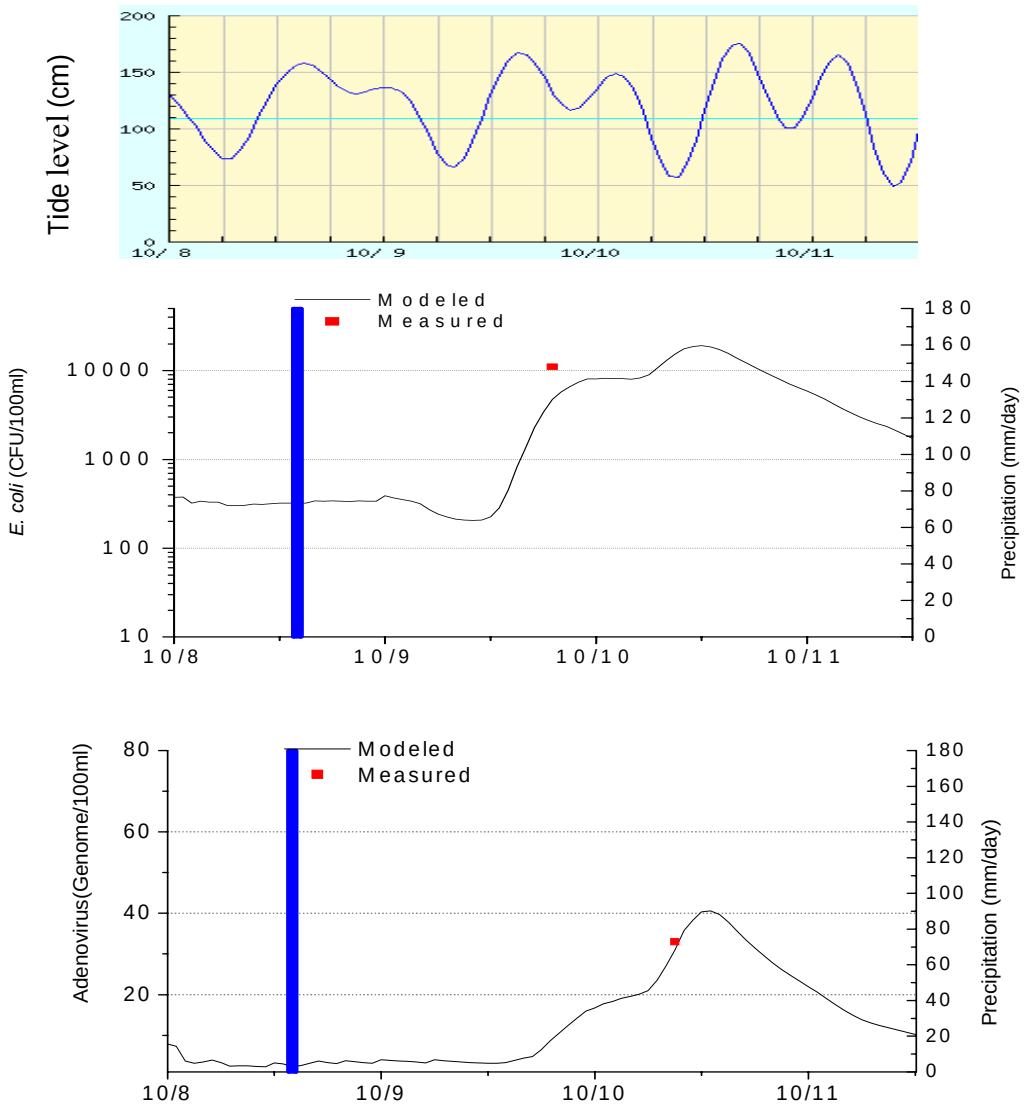

Fig. 4.25. Effect of rainfall and tides for Pathogen variations under the large storm event at St.4

CHAPTER 5: DISCUSSION

5.1 Field Observation

Influence of rainfall and the associated CSO was observed by field sampling. The water quality parameters, water nutrients and pathogen level in the water column were found to be highly variable. The water quality and water nutrients observation was done to understand the general trend and to use as a supportive data. The main emphasis was given to pathogen and *E. coli* and AdV was used as an indicator of rainfall induced CSO contamination.

The pathogen concentration exhibits significant spatial and temporal structure at scales not resolved by present monitoring programs. This is generally consistent with the findings of other researchers for other water bodies (e.g., Shibata *et. al*., 2004; Whitman and Nevers, 2004; Hellweger and Masopust, 2008). The observed data indicated the presence of pathogen plume associated with the wet weather. Pathogen level increased significantly after rainfall. However, the pathogen data collected to quantify the source was rather too little.

The highly variability of indicator contaminants over time is not unlikely in the area like Odaiba, where there would be continuous mixing and transport of contaminants along with the flow. Therefore collecting a single daily sample would not adequately characterize the dynamics and distribution of contaminants. To avoid or to minimize this uncertainty, high frequency sampling is necessary. But frequent sampling and monitoring is very difficult. To avoid this, a numerical modeling is done as a potential alternative to monitoring. Hellweger and Masopust, 2008 also pointed out the same things in their modeling of *E. coli*.

However, accurate and ample field data are necessary for adequate calibration of a numerical model. The field sampling performed in the Odaiba area of Tokyo Bay on November, 2007 was not adequate to calibrate the model. So, secondary data taken during 2004 was used to calibrate the model.

5.2 Numerical Modeling

CSOs contribute high pollutant loads, relative to dry weather flows, but for short periods of time and at randomly distributed intervals. Concern has arisen about the relative impact of these pollutant sources on coastal water quality. The effects on the flow distribution and water quality within Tokyo Bay have been investigated by the development and refinement of a three-dimensional hydrodynamic, water quality and pathogen model which includes inputs mainly from river drainage and CSOs from STPs and pumping stations located near the study area. The present model predictions have generally shown good agreement between measured field data and calculated data in all three stations.

It was found that concentrations of Pathogen vary widely according to space and time. The density distributions produced by the balance of tides and discharges from river and STPs have very complex effects. The big storms with CSO discharge were occurred on August 15 (32mm), August 29 (16mm), September 4 (106mm), October 5 (65mm) and October 9 (180mm) leaded to higher concentrations of pathogen. In contrast, a significantly higher plume was also found after a small rainfall (4mm) of August 23rd. This is significant, because it shows that high pathogen levels are not necessarily tied with amount of downpour. Even in small precipitations, pathogen significantly increased. Hellweger and Masopust, 2008 also found the same type of result during their *E. coli* modeling.

Fig. 4.24 shows after the small rainfall event (16mm) on August 29, the levels of *E. coli* increased rapidly due to mainly discharges from the Sunamachi and Chibaura STPs (located at the upper bay near Odaiba area, see Fig.3.1). In contrast, under the largest rainfall event on October 9 (180mm) did not increase the level so much in compare with smaller rainfall events due to mixing and tidal force. These kinds of results would be impossible to understand only from observation. The model successfully captured complex distributions of pathogen and helped our understanding of pathogens contaminations.

The predicted pathogen levels were higher for spring tides than for neap tides. During a spring tide, the effluent plume from the lower bay spread faster and reaches Odaiba area. Even in a dry weather conditions little bit increased concentration occurred for a spring tide, whereas for wet weather conditions, the neap tide results showed an increase in the pathogen concentrations at all the stations. For dry weather conditions, the pathogen loads originated mainly from the river Sumida, whereas for wet weather conditions, the main load came from the pumping stations. During dry weather conditions, the predicted pathogen concentrations were significantly below the mandatory standard required to comply with the bathing water standard. Kashefipour *et. al.,* 2002 also found similar type of result, when they studied in the Fylde Coast, UK.

There are however some significant discrepancies. The model captures that concentration decreases faster than the observed data. Calculation results shows usually after 2 days concentration decrease 1 order of magnitude, where as observation data shows that the higher plume sometime remains about a week (Fig. 4.14). Ackerman and Weisberg (2003) also found similar result after observation in Santa Monica Bay, California, US. They found bacterial concentrations returned to background levels in 5 days for all size of rain events. It may be because the increase is due to a more local effect, CSO discharge from upper river continues for longer time not included in the model.

The current standard for acceptably safe beaches for swimming set by of the Ministry of the Environment of Japan is a fecal coliform rate of 1000 coliforms unit per 100mL (CFU/100mL). According to US EPA this rate is even lower, 235 CFU/100mL. This index of fecal coliform includes not only *E. coli* but also others. However, it is well known that the majority of the fecal coliform in this area comes from *E. coli*. Therefore, we use a value of 1000 CFU/100ml *E. coli* as the standard for the safety of swimming in the sea. The calculation results reveal that most of the time of the storm prone period (August-September) of Japan violates standard for swimming.

Understanding the effects of physical factors is important to know the fate and distributions of pathogens. Such an understanding is in turn highly related to the assessment of sanitary risks in urban coastal zones. Occasional elevated pathogen level due to storm induced CSO have been causing the bathing waters of Odaiba failed to comply with the mandatory water quality standards (see Fig. 4.13). These failures have become one of the major threats to the local tourist industry. Many field measuring studies have been undertaking by various researchers in the Tokyo Bay. But these types of monitoring studies have been unable to provide robust quantitative data and thereby ascertain the impact of capital improvement schemes on the bathing water quality. Numerical experiments were thus conducted to examine the variations in rates of *E. coli* and AdV according to time and space.

The *E. coli* concentration and associated loading from streams can be affected by numerous factors, including runoff and discharge and resuspension from the sediment bed (Olyphant *et. al*., 2003; Haack *et. al*., 2003). It was investigated whether resuspension phenomenon was happened during study period or not. From the observation data (Fig 3.8) it was found that though there was no antecedent rainfall, concentration of *E. coli* increased up to 1000 CFU/100 ml at St.3 and St. 5 in August 12th. Though, this phenomenon was not seen in case of AdV (Fig. 3.9).

It is well known that pathogen can attach with sediment. So pathogen concentration is positively related with particle resuspension which is as a function of wind speed. Wind has a direct effect on the suspended matter concentration in the shallow (<2 m) water above the tidal flats, but not necessarily in the water of the deep (7-25 m) main channels (Jonge and Beusekom, 1995). In shallow environments, under certain conditions of fetch, wind velocity, bathymetry and bottom characteristics, resuspension can be generated by wind induced waves. Only austral trade winds with a speed >3 m s^{-1} allow particle resuspension which is effective for depths<1.5 m (Robert *et. al*., 1994). According to Arfi *et. al*. (1993), the wind speed for resuspension seemed to be >3 m s^{-1} for water depth of 1.0-1.2 m and bottom shear stress > 0.5 N m^{-2}. Sediment resuspension may occur at wind speeds exceeding 6–8 m s^{-1} for a water depth of 3m could contribute significantly to enterococci conc in the overlying water (Roselev *et. al*., 2008).

So it is clear that resuspension process depends mainly on wind speed and water depth. The observation data (Fig 3.4) shows that at that time wind velocity was about 7m/s. and the depth of the study area (St 3 = 11m and St 5 = 14m) was also higher. So it needs very strong wind for resuspension at St 3 and 5. As wind was not so strong during sampling time, the suspected resuspension might not be happened during the particular time. So resuspension effect was not included in the model.

Similar phenomenon of abnormal increase of *E. coli* (Fig. 3.8) again found during September 22nd. Though at that time 4.5 mm rainfall was observed (Table 3.4) along with 11 m/s and 8 m/s wind flow at November 21st and November 22nd respectively. Ackerman and Weisberg, 2003 studied on the relationship between rainfall and beach bacterial concentrations on Santa Monica beaches, CA, USA. They found that every storm larger than 25 mm and 91 percent of the rain events between 6 mm and 25 mm resulted in an increase in the number of sites failing water quality standards. Where as for storms smaller than 2.5 mm, there was almost no increase. So as it was 4.5 mm rainfall at September 22nd, it is not clear whether the increase *E. coli* concentration was happened due to rainfall, resuspension or any other unidentified sources.

The modeled result (Fig. 5.1) shows that occurrence of *E. coli* did not correlate well with that of AdV. It may be due to the difference in discharge input and survival rate in water column. This is also consistent with the findings of Jiang *et. al*. (2007). They found in their study that occurrence of human entroviruses did not correlate with that of Fecal Indicator Bacteria. Fong *et. al. (*2004) also pointed out that Coliform standard often fail to predict the occurrence of many waterborne human pathogens.

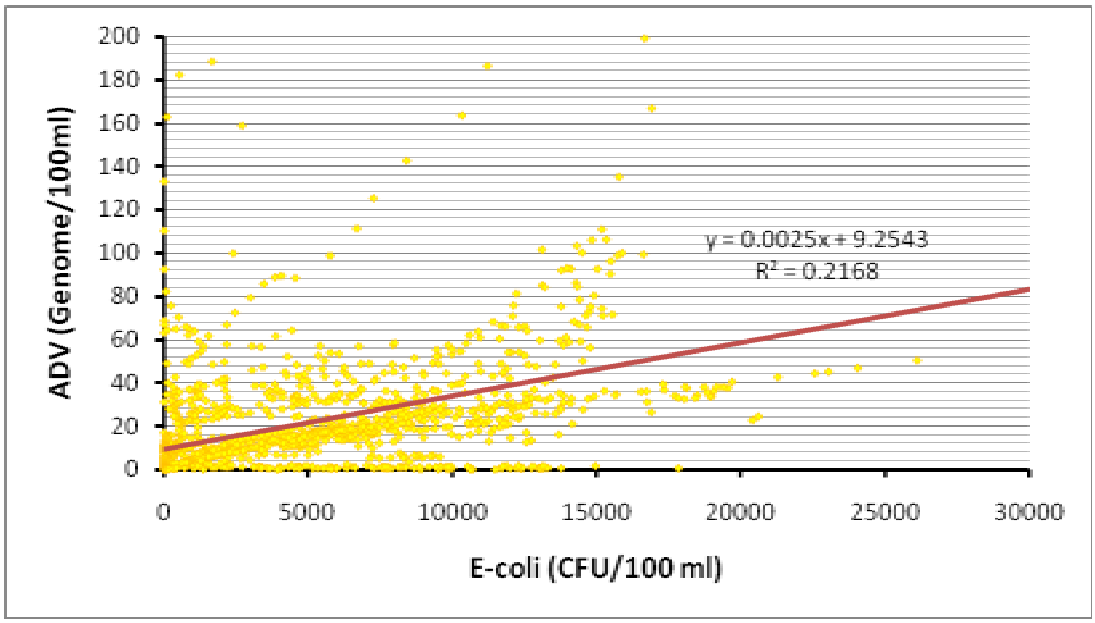

Fig. 5.1. Relationship between simulated E. coli and AdV

5.3 Potential Model Improvements

Although the model reproduces the major features of the spatial and temporal pathogen patterns, there is room for improvement. Major uncertainties are likely in the time-variable inflow concentration (i.e., first flush), other sources (direct runoff), variable die-off rate (solar radiation), settling and storage in the sediment bed. In this model a constant input of pathogen and constant die-off rate is used for lack of time-variable data.

As there was no evident of resuspension in the study area, the model does not include resuspension effect due to currents and wind waves. However, to use this model in the other area with a broader aspect, some model development would be required to account for sediment transport linked with pathogen component. Incorporating sunlight-dependent die-off will also likely require accounting for spatially and temporally variable light extinction.

Additional calibration and/or validation over a longer period would also be beneficial, which would require more data collection. This should include additional pathogen density surveys as well as hydrodynamic data.

CHAPTER 6: CONCLUSIONS & RECOMMENDATIONS

6. 1 Guideline and Recommendation

From the literature review (chapter 2.6) it is found that,

1. Separation of sewer is difficult, expensive and not practical.
2. Construction costs of big volumes storage for large storm are very high and are highly dependent on geography, geology, and land use condition.

From the present modeling results it is clear that,

1. Distribution and dynamics of pathogens is very complex. So it is very difficult to make forecast warning effectively for the beach swimmers.
2. Small size of rainfall events can also cause significant increase of pathogen load to the bay water.
3. Larger storm event is not so frequent and loadings from larger storms usually represent only a small fraction of the total annual CSO. and

So considering all the above mentioned facts, it can be recommended that,

1. Utilization of relatively small volumes of low cost retention storage tank can be effective in retaining pollution loadings from small, frequent storm events.
2. Small size of storage system (200 to 400 cubic feet per acre) can effectively address much of the CSO problem (NRC, 1993). The Kisshoin Trunk Sewer in Kyoto, Japan have a storage capacity of 13000 m^3 can store 5mm/hr rainfall (Morita Hiroaki, 2003). It can also store first flash of a big storm. How to and where to construct a storage tank has shown in chapter 2.6 of literature review.
3. For big storm case, awareness should create to avoid swimming. All kind of beach activities should be restricted until at least 3 days following a big storm.
4. Once the small rain can be protected by installing reservoir facilities, then only consider about big storms. Otherwise people have to restrain from swimming both after small and big size of storms.

6.2. Summary and Conclusion

The present study observed the spatial and temporal patterns of pathogen in the Odaiba area, Tokyo Bay. The pathogen levels in the water column were found to be quite variable spatially and temporarily. And there is not a consistent relationship between rainfall or input and elevated pathogen concentrations. Outfalls may discharge rapidly and consistently after major storms, but the transport of the plume to another location variable with time, depending on hydrodynamic and tidal conditions.

A mechanistic coupled hydrodynamic and water quality model was constructed, which can reproduce the general spatial and temporal patterns of *E. coli* and AdV in the Tokyo bay. The model demonstrated that the pumping stations located near the study area are the predominant source of pathogen to the bay. In a similar manner, Liu *et. al.* (2006) used a model to demonstrate that the water quality at a beach located between two pollutant sources can be influenced by either source, depending on the current direction. McCorquodale *et. al.* (2004) also used a model to demonstrate that instream transport can change significantly depending on the hydrodynamic conditions.

The distributions and dynamics of pathogen were found very complex. Modeling result shows that high pathogen levels are not necessarily consistent with amount of rainfall. Even small precipitations can cause significant increase of pathogen concentration especially in the near shore areas. So small precipitation event should also be considered in developing management plan of coastal waters.

This study demonstrated the utility of hydrodynamic and water quality modeling for predicting spatial and temporal patterns of *E. coli* and AdV in the water body of Odaiba. The factors affecting pathogen concentration will vary from system to system, but this study demonstrated that high-resolution spatial and temporal patterns observed in *E. coli* and AdV can be explained using present modeling technology. This technology should be considered as a potential alternative to the nearly impossible intensive monitoring, when constructing management systems.

The model can be significantly improved by extending the range of conditions used for calibration and doing several model improvements (discussed above). Monitoring of pathogen at STPs and inflowing River discharges at daily or higher temporal resolution should provide the data to support and validate the improved model.

Considering water quality in general, and pathogen concentration in particular as an additional objective could be beneficial. Releases via pumping station could, for example, be done at night, to prevent drawing the pumping stations and connected rivers plume into the recreational area of Odaiba sea beach during the day. Establishment and management of storage tanks or reservoirs based on multiple objectives is very worth full. Relatively small size of storage can be effective to address most of the CSO problem caused by small and frequent storm events. Which is also effective to treat the polluted most first flush. And for larger storm event, it can be created awareness among sea goers, or ban swimming in the beach until after 3 days of big storm.

CHAPTER 7: REFERENCES

Ackerman, D., and S. B. Weisberg, 2003. Relationship Between Rainfall and Beach Bacterial Concentrations on Santa Monica Bay Beaches. Journal of Water and Health, 01.2. pp 86.

Arfi, R., Guiral, D. and M. Bouvy, 1993. Wind Induced Resuspension in a Shallow Tropical Lagoon. Journal of Estuarine, Coastal and Shelf Science, 36,587-604.

Asad H. M., 2006. Numerical Simulation of Residual Currents and Water Quality in Semi-Enclosed Bays. Ph.D. Dissertation, Dept. of Socio-cultural Environmental Studies, GSFS, University of Tokyo, Japan.

Balarajan, R., V. Soni Raleigh, P. Yuen, D. Wheeler, D Machin, and R. Cartwright, 1991. Health risks associated with bathing in sea water. Br. Med. J. 303:1444–1445.

Barbé, D. E., Carnelos, S., and McCorquodale, J.A., 2001. Climatic Effect on Water Quality Evaluation. Journal of Environmental Science and Health, A36 (10), 1919-1933.

Blumberg, A. F., and Mellor, G. L., 1987. A Description of a Three-dimensional Coastal Model. Three Dimensional Coastal Ocean Models, N. S. Heaps, ed., American Geophysical Union, Washington, D.C., 1-16.

Boehm, A.B., S.B. Grant, J.H. Kim, S.L. Mowbray, C.D. McGee, C.D. Clark, D.M. Foley, and D.E. Wellman, 2002. Decadal and Shorter Period Variability of Surf Zone Water Quality at Huntington Beach, California. Environmental Science and Technology 36(18):3885-3892.

Bosch, A. 1995. The survival of Enteric Viruses in the Water Environment. Microbiologia SEM 11:393–396.

Boussinesq, J., 1903. *The'orie analytique de la chaleur*, Vol. 2, Gauthier-Villars, Paris.

Bureau of Sewerage, TMG (Tokyo Metropolitan Government), 2005. Annual Report of Sewerage in Tokyo. Available (in Japanese) at http://www.gesui. metro.tokyo.jp/.

CDC (Centers for Disease Control), 2004. Healthy Swimming. Center for Disease Control, Atlanta, Georgia. http://www.cdc.gov/ healthyswimming/index.htm, accessed December 14, 2007.

Connolly, J.P., Blumberg, A.F., and Quadrini, J.D., 1999, Modeling Fate of Pathogenic Organisms in Coastal Waters of Oahu, Hawaii. Journal of Environmental Engineering, Vol. 125, No. 5.

Enriquez, C. E., C. J. Hurst, and C. P. Gerba. 1995. Survival of the Enteric Adenoviruses 40 and 41 in tap, sea, and waste water. Water Res. 29:2548– 2553.

Fong, T. T., Griffin, D. W., Lipp, K., 2005. Molecular Assays for Targeting Human and Bovine Enteric Viruses in Coastal Waters and Their Application for Library-Independent Source Tracking. Applied and Environmental Microbiology, p. 2070–2078.

Fordiani, R., 2006. CSO Control Technologies, Omaha CSO Control Program, Published on the website *(http://www.iawpca.org).*

Furukawa, K., 2003. Water Flows in Tokyo Bay: Fascinating Aspects, Special Features: Water management

Gabriel, B., 2005. Public Health Aspects of Waste Water and Biosolids Disposal in the Marine Environment. Depertment of Environmental Engineering Sciences, Florida, USA.

Gerba, C. P., D. M. Gramos, and N. Nwachuku. 2002. Comparative inactivation of enteroviruses and adenovirus 2 by UV light. Appl. Environ. Microbiol. 68:5167–5169.

Gommes, R., J.du Guerny, F. Nachtergaele and R. Brinkman, 1998. Potential Impacts of Sea-level Rise on Populations and Agriculture, Food and Agriculture Organization of the United Nations, published on the website *(http://www.fao.org/sd/eidirect/EIre0046.htm).*

Griffin, D.W., Donaldson, K.A., Paul, J.H. and Joan B. R., 2003. Pathogenic Human Viruses in Coastal Waters. Clinical microbiology reviews, jan. 2003, p. 129–143.

Haack, S.K., L.R. Fogarty, and C. Wright, 2003. *Escherichia coli* and Enterococci at Beaches in the Grand Traverse Bay, Lake Michigan: Sources, Characteristics, and Environmental Pathways. Environmental Science and Technology 37:3275-3282.

Harris, E.L., R.A. Falconer and B. Lin, 2004. Modelling Hydroenvironmental and Health Risk Assessment Parameters along the South Wales Coast. Journal of Environmental Management 73 (2004) 61–70.

Hellweger, F. L. and Petr M., 2008. Investigating the Fate and Transport of Escherichia Coli in the Charles River, Boston, using High-resolution Observation and Modeling. Journal of the American Water Resources Association. Vol. 44, No. 2. Pp 510.

Hosokawa, Y., 2003. Toward a pleasant, beautiful Tokyo Bay, Special Features: The Environment Integrated Report, Baton Rouge, Louisiana.

Japan Scientists Association, 1979. The Tokyo Bay. In: Kondo, K. (Ed.), The Past and Present in Tokyo Bay. Tokyo, p. 2 (in Japanese)

Jiang, S.C., Weiping C., and Jian,W. H., 2007. Seasonal Detection of Human Viruses and Coliphage in Newport Bay, California. Applied and Environmental Microbiology, Oct. 2007, p. 6468–6474.

Jonge V. N. and Beusekom J. E. E., 1995. Wind and tide-induced resuspension of sediment and microphytobenthos from tidal flats in the Ems estuary. Journal Lmnol. Oceanogr. 40(4), 1995, 766-778.

Kantha, L.H. and Clayson, C.A., 2000. Numerical models of oceans and oceanic processes, Academic Press, International Geophysics Series, ISBN: 0-12-434068-7.

Kashefipour, S.M., B. Lin, E. Harris, R.A. Falconer, 2002. Hydro-Environmental Modelling for Bathing Water Compliance Ofan Estuarine Basin. Water Research 36 (2002) 1854–1868.

Koibuchi, Y. and Isobe, M., 2001. Temporal and spatial dynamics of water quality on Ariake Bay during the year of 2001, Proc. Coastal Engg. JSCE, 49, pp. 1056-1060.

Konovsky J., Levi K., and J. Puhn, 2006. Influence of Wind on Resuspension of Bacteria on Intertidal Sediment in Oakland Bay, US. Poster presentation on the website (*http://www.co.mason.wa.us).*

Kueh, C. S. W., T.-Y. Tam, T. Lee, S. L. Wong, O. L. Lloyd, I. T. S. Yu, T. W. Wong, J. S. Tam, and D. C. J. Bassett, 1995. Epidemiological Study of Swimming-associated Illnesses Relating to Bathing-beach Water Quality. Water Sci. Technol. 31:1–4.

Lick, W., Lick, J. and Ziegler, C.K., 1994. The Resuspension and Transport of Fine-Grained Sediments in Lake Erie. J. Great Lakes Res., 20(4), 599-612.

Lipp, E. K., R. Kurz, R. Vincent, C. Rodriguez-Palacios, S. R. Farrah, and J. B. Rose, 2001. The Effects of Seasonal Variability and Weather on Microbial Fecal Pollution and Enteric Pathogens in a Subtropical Estuary. Estuaries 24:238–258.

Liu, L., M.S. Phanikumar, S.L. Molloy, R.L. Whitman, D.A. Shively, M.B. Nevers, D.J. Schwab, and J.B. Rose, 2006. Modeling the Transport and Inactivation of E. coli and Enterococci in the Near-Shore Region of Lake Michigan. Environmental Science and Technology 40:5022-5028.

Maki, H., Hiroyuki S., Takehiko H., Hiroshi K., Kunio K., Masao Y., Toshio K., Haruo A., and Watanabe M., 2007. Influences of Storm Water and Combined Sewage Overflow on Tokyo Bay. Environmental Forensics, 8:173-180, 2007.

Managaki, S., Hideshige T., Dong-Myung K., Toshihiro H., and Shiraishi H., 2006. Three Dimensional Distributions of Sewage Markers in Tokyo Bay Water—Fluorescent Whitening Agents (FWAs), Marine Pollution Bulletin 52 (2006) 281–292.

Marsalek, J. and Quintin, R., 2004. Urban wet-weather flows: sources of fecal contamination impacting on recreational waters and threatening drinking-water sources. Journal of Toxicology and Environmental Health, Part A, 67:1765–1777, 2004

McCorquodale, J.A., Georgiou, I., Chilmakuri, C., Leal, J., Martinez, M., and Englande, A.J., 2005, Modeling Circulation, Pathogen Fate and Transport in Storm Water Plumes on the North Shore of Lake Pontchartrain, Louisiana. Submitted to National Oceanographic Atmospheric Administration of United State. p. 57.

Metcalf and Eddy, Inc., 2003. Wastewater Engineering, Treatment and Reuse (Fourth Edition). McGraw-Hill, Boston, Massachusetts.

Miossec, L., F. Le Guyader, L. Haugarreau and M. Pommepuy. 2000. Magnitude of rainfall on viral contamination of the marine environment during gastroenteritis epidemics in human coastal population. Rev. Epidemiol. Sante´ 480398–7620:2S62–2S71.

Morita Hiroaki, 2003. Present Status of Combined Sewer Overflow and New CSO Control Policy in Japan. Waste Water System Division, Water Quality Control Department, National Institute of Land and Infrastructure Management, 1, Asahi, Tsukuba, Ibaraki, 305-0804, Japan.

MWRDGC (Metropolitan Water Reclamation District of Greater Chicago), 2006. Protecting Our Water Environment, Combined Sewer Overflow Public Notification Plan, Revised January 2006. http://www.mwrdgc.dst.il.us/MO/csoapp/cso.htm.

NRC (National Research council), 1993. Managing Wastewater in coastal Urban Areas. National Academy press, Washington, D.C., USA.

Nobles, R. E., P. Brown, J. Rose, and E. Lipp. 2000. The investigation and analysis of swimming-associated illness using the fecal indicator *Enterococcus* in Southern Florida's marine water. Fla. J. Environ. Health 169:13–19.

Olyphant, G.A. and R.L. Whitman, 2004. Elements of a Predictive Model for Determining Beach Closures on a Real Time Basis: The Case of 63rd Street Beach Chicago. Environmental Monitoring and Assessment 98:175-190.

Olyphant, G.A., J. Thomas, R.L. Whitman, and D. Harper, 2003. Characterization and Statistical Modeling of Bacterial (Escherichia coli) Outflows From Watersheds That Discharge Into Southern Lake Michigan. Environmental Monitoring and Assessment 81(1-3): 289-300.

Onozawa, K., 2005. Bachelor Dissertation, Dept. of Urban Engineering, University of Tokyo, Japan (In Japanese).

Onozawa, K, Koibuchik Y, Furumai, H, Katayama, H, Isobe, M., 2005. Numerical Calculation of Combined Sewer Overflow (CSO) Due to Heavy Rain Around Daiba in the Head of Tokyo Bay. Annual Journal of Coastal Engineering, JSCE 52:891-895 (in Japanese).

Prudman, J., 1953. Dynamical Oceanography, Methuen & Co., London, pp 409.

Radjawane, I. M., Matsuyama,, M., Kitade, Y. and Suzuki, T., 2001. Numerical Modeling of Density-driven Current in Tokyo Bay. La Mer 39, pp. 63-75.

Robert a., Daniel g. And m. Bouvy, 1994. Sedimentation Modified by Wind Induced Resuspension in a Shallow Tropical Lagoon (cote d'ivoire). Netherlands Journal of Aquatic Ecology 28(3-4) 427-431.

Roslev, P., Bastholm , S. and & I. Niels, 2008. Relationship Between Fecal Indicators in Sediment and Recreational Waters in a Danish Estuary. Journal of Water Air Soil Pollut, 194:13–21.

Sasaki, J. and M. Isobe, 1996. Development of a long-term predictive model of water quality in Tokyo Bay, Proc. Estuarine and Coastal Modeling, ASCE, pp. 564-580.

Shibata, T., H.M. Solo-Gabriele, L.E. Fleming, and S. Elmir, 2004. Monitoring Marine Recreational Water Quality Using Multiple Microbial Indicators in an Urban Tropical Environment. Water Research 38(13):3119-3131.

Sinton LW, Hall CH, Lynch PA and RJ Davies-Colley, 2002. Sunlight Inactication of Fecal Indicator Bacteria and Bacteriophages from Waste Stabilization Pond Effluent in Fresh and Saline Waters. Appl Environ Microbiol 68:1122-1131.

Straub, T. M., and D. P. Chandler, 2003. Towards a Unified System for Detecting Waterborne Pathogens. J. Microbiol. Methods 53:185–197.

Sugita, T., Kurozumi, M., Ohashi, H. and H. Mizushima, 2003. Feasibility Study on the Real-time Control System of the Pumps for the Reduction of Combined Sewer Overflows. Annual Report on Technical Research & Development. Bureau of Sewerage, Tokyo Metropolitan Government, (2003) p. 459-476.

Thurston-Enriquez, J. A., C. N. Haas, J. Jacangelo, and C. P. Gerba**,** 2003. Chlorine Inactivation of Adenovirus Type 40 and Feline Calicivirus. Appl. Environ. Microbiol. 69**:** 3979–3985.

USEPA (U.S. Environmental Protection Agency), 2003. EPA's BEACH Watch Program: 2002 Swimming Season. EPA 823-F-03-007. U.S. Environmental Protection Agency (USEPA), Washington, D.C.

USEPA (U.S. Environmental Protection Agency), 2004. National Water Quality Inventory. US Environmental Protection Agency (EPA), Washington, D.C. http://www.epa.gov/305b/ 2000report/, accessed December 14, 2007.

Wetz, J. J., E. K. Lipp, D. W. Griffin, J. Lukasik, D. Wait, M. D. Sobsey, T. M. Scott, and J. B. Rose, 2004. Presence, Infectivity, and Stability of Enteric Viruses in Seawater: Relationship to Marine Water Quality in the Florida Keys. Mar. Pollut. Bull. 48:698–704.

Whitman, R.L. and M.B. Nevers, 2004. *Escherichia coli* Sampling Reliability at a Frequently Closed Chicago Beach: Monitoring and Management Implications. Environmental Science and Technology 38(16):4241-4246.